Complex retreat behavior in experimental barrier island response to base level rise

A THESIS

SUBMITTED TO THE FACULTY OF THE

UNIVERSITY OF MINNESOTA

BY

Nicholas Rodgers

IN PARTIAL FULFILLMENT OF THE REQUIERMENTS

FOR THE DEGREE OF

MASTER OF SCIENCE

Dr. Chris Paola, Advisor

August 2019

Acknowledgments

First and foremost, I need to thank my advisor, Chris for everything he has done for me. Thank you for taking a risk by accepting a fresh-faced geologist from Ohio. Not only did you graciously bring me into your world of water and sediments; you did so with an enthusiasm that could turn anyone into a fluid dynamics fanatic. Thank you for always being willing to discuss topics I was stuck on and making sure I was on the right track. Besides helping me work through my research and thesis, you showed me what kind of scientist I want to be through your curiosity, kindness, and openness.

This work could not have happened without the incredible staff at SAFL. Prior to this project, I was blissfully unaware of how many problems arise during experiments. From helping me figure out the dials and knobs of SAFL to repairing lasers after heavy use, the staff helped me every step of the way. A special thank you to Ben Erickson, Aaron Ketchmark, and Erik Steen who I relentlessly pestered with questions and problems.

Thank you to everyone who passed though the Paola group at some point during my time here, especially Gerard Salter, Dan Cazanacli, Elisabeth Steel, Alicia Sendrowski, and Ajay Limaye. Your discussions and feedback made this work better in every way. Thank you to my support network both here in Minnesota and back at Ohio State. Geology is pretty cool but it's better with friends. And lastly, I'd like to thank my girlfriend Jen who supported me the whole way and has probably heard enough about experimental deltas for one lifetime.

Dedication

To my parents, who instilled a love of nature in me early on and endlessly supported my curiosity, even when it brought me to this strange place called Minnesota.

Son's Research Haiku – Eileen Rodgers

Sediment piling

Wave action, water flowing

Oh look an island

Table of Contents

List of Tables

List of Figures

1 Introduction

At the end of the Last Glacial Maximum (LGM) global sea levels began to rise pushing shorelines and river mouths inland. Along some coasts, waves had collected sediment in large shore-parallel sandbars. Once relative sea level (RSL) began increasing, these bars separated from the mainland as the low areas around the bars were flooded. Since the end of the LGM, sea level has continued to increase, and these former sandbars have responded by moving inland to keep up with the rising seas.

In the last few thousand years, RSL rise rates have decreased and barrier islands have stabilized and are found along 10% of the world's oceanic coastlines today (Stutz & Pilkey, 2011). Barrier islands protect areas from ocean waves to create interior lagoons and wetlands, important environments for many species, especially those avoiding the predators of the mainland (Burger & Lesser, 1978). Humans have utilized barrier islands for recreation and fishing as well as building on and behind the islands.

24% of all barrier islands are found in the United States and important parts of United States history took place on these islands. Before English explorers arrived at the Outer Banks, North Carolina, there were Native American people using the land. The Algonquian people used the barrier islands for both farming and fishing. Unfortunately, like so many Native Americans, the Algonquians were not immune to the diseases that the English settlers brought with them and their numbers fell drastically (Downing, 2013). When the first permanent settlements were established on the Outer Banks in the

late 17th century, an unexpected trouble arose: piracy. The isolation of the barrier islands did not just attract animals evading predators, the islands served as havens for those looking to avoid the law of the mainland. One particularly infamous pirate Edward Teach, or "Blackbeard" used the Outer Banks as his base of operation while he pillaged trading vessels. Blackbeard was such a hinderance on the area that his death marked the end of the golden age of piracy and allowed for the continued settlement of the Outer Banks (Stick, 2015).

The islands continued to be somewhat isolated for the next century. The fishing industry was viable for those who lived on the islands but the difficulty of transporting goods back to the mainland meant that most of the catch remained on the islands. This created a very self-sustained economy where goods produced by the islands were used on the islands. The island economies were so water-tight that the addition of just two visitors by the names Wilbur and Orville Wright massively disrupted one island's economy (Wright, McFarland, Chanute, & Wright, 1953). These brothers would forever change the Outer Banks after their first flight at Kitty Hawk; people began visiting the island to see the historic site (White, 2008). This increase is tourism lead to massive development on the islands, especially around Kitty Hawk. This development culminated in the completion of the "Wright Memorial Bridge" which finally connected the islands to the mainland increasing ease of access for would-be tourists ("Wright Memorial Bridge," 1932). Today more than 2 million people visit the Outer Banks each year (NPS, 2017). Unfortunately, rising seas and storms pose a threat to barrier islands. Losing barrier

islands would mean the loss of these historic places as well as damage to important natural environments.

It is not just the Outer Banks that are in danger, all over the world climate change is intensifying the dangers barrier islands face. RSL rise can drown barrier islands, which are rarely more than a few meters above sea level. Along with RSL rise, the frequency of tropical storms is increasing (Emanuel, 2013) and wave power has been increasing in recent years (Losada, Reguero, Losada, & Méndez, 2019). These factors make it possible for water to overtop barrier islands. Once that happens overwash can occur where the overtopping water transports sediment from the ocean side of the island to the lagoon side. Overwash is believed to be the mechanism by which barrier islands can move upslope to avoid drowning (Leatherman, 1979; Lorenzo-Trueba & Ashton, 2010; Moore, List, Williams, & Stolper, 2010).

Studying barrier island behavior in the field is challenging because of the long timescales on which the islands evolve. Field barriers are stable at current RSL rise rates, and storm events are unpredictable. Physical experiments are valuable because they allow us to study barrier island processes in a controlled environment and at an accelerated pace.

Barrier islands are often found along the fringes of wave-dominated deltas. The deltas provide the necessary sand and the wave climate transports that sand. Some examples of deltas with barrier islands are the Danube, Po, and Selenga river deltas. We attempted to create experimental wave dominated deltas to form barrier islands in the lab.

Chapter 2 of this thesis outlines the methodology and results of these physical experiments. These experiments include 4 separate runs where delta slope and RSL rise rate were varied. We collected overhead images and topography from a laser scanner and these were analyzed to determine how barrier islands respond to RSL rise. Chapter 3 is a summary of the results as well as possible future work inspired by this project.

2 Complex retreat behavior in experimental barrier island response to base level rise

Synopsis

Barrier islands act as natural barriers between the ocean and the mainland. These islands create protected, low energy environments behind them that are important ecological and economic hubs. Barrier islands are naturally low-laying features and are susceptible to drowning from sea level rise. However, previous work suggests that barrier islands can retreat upslope to keep up with sea level rise and maintain their subaerial extent. To explore this idea, we performed physical experiments where barrier islands were subjected to a constant relative sea level rise (RSL) and constant wave environment. We tracked the islands through time with overhead images and periodic laser elevation scans. Time series of island location show that the islands did not retreat at constant rates through the transgression. Rather, overall long-term retreat occurred through a "stick-slip" motion comprising stationary intervals alternating with backward steps. The source of this complex behavior is a cycling between two morphologies: one where an island has a developed ridge and another where no ridge is present. Sea level rise allows waves to overtop the island and erode the ridge that once kept the waves at bay. That sediment is deposited behind the island, moving the barrier landward. Waves continue to push sediment back towards the mainland until the island becomes too wide for waves to carry sediment all the way across the island. This begins a process of backfilling the overwash fan, eventually creating a new ridge. These simple experiments support previous

theoretical suggestions that periodic overwash is a key part of a barrier island's behavior during a transgression, and that this can lead to punctuated retreat even when RSL rise is steady.

1 Introduction

Barrier islands are low-lying, shore-parallel features found along 10% of the world's oceanic coastlines (Stutz & Pilkey, 2011). These islands are critical parts of the coastal systems where they are present; they create interior lagoons and wetlands, sheltered from large wave, that are highly biologically productive; and they provide important nesting areas for many seabirds, separate from the mainland and mammal predators (Burger & Lesser, 1978). In addition to using them extensively for recreation and fishing, humans have built on and behind barrier islands because the islands offer protection from waves and large storm events. These low energy lagoons rely on the protection of the islands to maintain salinity and low wave energy. Barrier islands can form anywhere with sufficient sand and wave energy to transport it. Deltas often provide abundant sand so wave dominated deltas such as the Danube, Po, and Selenga river deltas form barrier islands along their shorelines. These locations are ideal for barrier island formation because the deltas supply the sand necessary for the islands and the waves collect that sand in piles along the shoreline.

Barrier islands do not typically rise more than a few meters above mean sea level and thus seem susceptible to drowning from sea level rise and storm events. The loss of

barrier islands due to rising relative sea level (RSL) would be catastrophic on many coastlines, both from the natural-environment and human perspectives.

Climate change is dangerous to barrier islands in a variety of ways; sea level rise has the possibility to drown barrier islands, the frequency of tropical storms is increasing (Emanuel, 2013), threatening to destroy barrier islands, and the overall power of waves has been increasing in recent times (Losada et al., 2019). As water levels rise and allow waves to overtop these islands, a process called overwash can occur in which sediment is transported from the shoreface of the island to the lagoon. This process moves the overall center of mass of the island landward and potentially allows the barrier to move upslope to prevent drowning.

Studying barrier island behavior in the field is challenging because of the long timescales on which the islands evolve. At current rates of sea level rise, any tendency to drown is hard to distinguish from natural variability, and storm events are unpredictable in frequency and intensity. At the start of Holocene time, barrier islands in North America and Europe were migrating landward but as the rate of RSL rise decreased in the last few thousand years, the barrier islands slowed their retreat or even stabilized (Beets & Van Der Spek, 2000; Leatherman, 1983; Stapor et al., 1991). To provide additional insight, here we report results from physical experiments that allow us to study the equivalent of many years of sea level rise effects in a reasonable amount of time. The experimental barriers were supplied with sediment via a delta.

Previous studies of barrier island systems and their response to sea level rise have ranged from field observations to numerical modeling (Houser, 2012; Leatherman, 1979; Lorenzo-Trueba & Ashton, 2010; Moore et al., 2010; Swift, 1975). Many of these studies found that overwash is the mechanism by which barriers retreat inland. Some studies use barrier island deposits to understand past RSL rise rates, storm climates, or sediment budgets (Ciarletta, Shawler, Tenebruso, Hein, & Lorenzo-Trueba, 2019; Donnelly & Woodruff, 2007; Sanders & Kumar, 1975; J. Shaw, You, Mohrig, & Kocurek, 2014). We were especially interested in investigating the finding of Lorenzo-Trueba and Ashton that barrier islands can retreat at a non-constant rate under a constant sea level rise rate.

2 Methods

2.1 Experimental Set-up

We performed a series of four experiments in a delta basin at Saint Anthony Falls Laboratory at the University of Minnesota. The delta basin is an experimental tank used to create river deltas while precisely controlling base level, river water and sediment supply, and wave climate. The tank itself is a 5-meter by 5-meter watertight basin with a depth of 0.5 meters (Figure 1).

We fed a mix of water and sediment into one corner of the basin at controlled rates to build a quarter-circle delta. The sediment was a commercial walnut-shell sand, whose reduced density allows for lower delta-plain slopes and easier transport by laboratory-scale waves than quartz sand. The sediment has a specific gravity of 1.35 and was unimodal in size with a mean diameter of 0.5mm. The water (base) level in the tank

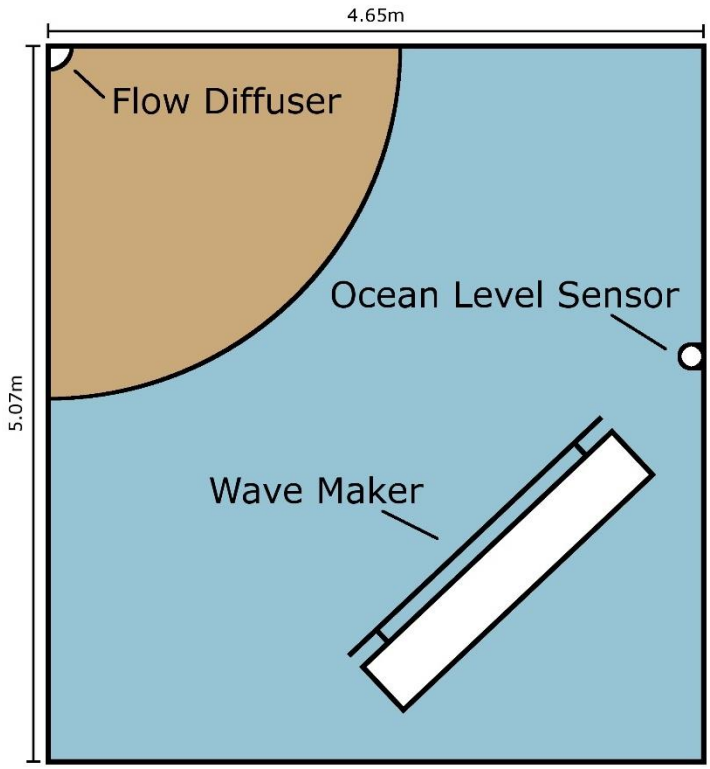

Figure 1: Schematic of the delta basin. Dimensions are 4.65m by 5.07m. Basin includes a corner flow diffuser where a water and sediment mixture are introduced as well as an ocean level sensor to keep track of the water level in the tank. The wave maker floats on the surface of the water near the opposite corner from the flow diffuser.

was measured every 5 seconds to a precision of 0.1 mm and could be increased or decreased during the experiment with a remotely controlled weir. Deltas were built with a constant water and sediment supply which created a constant slope along the delta top. The deltas were grown initially without the influence of waves to allow the largest possible starting radius. We introduced waves only after the delta was large enough to absorb a modest wave-induced transgression.

We created waves with a conventional paddle-type wave maker. The wave maker was in the basin corner across from the delta source and comprises a floating platform (to

allow the platform to follow changing base level), and an arm that oscillates to create monochromatic waves in the tank. Wave amplitude and period are adjustable over a wide range. The main control on wave energy delivered to the shoreline was intermittency of operation of the wave-maker rather than wave amplitude. The walls of the tank were lined with fiber batting to damp reflections.

2.2 Data Collection

We took overhead photos of the deposit every 10 to 30 seconds depending on the stage of the experiment. The camera used a wide-angle lens to capture the whole delta surface; as a result the lens distorted the images so we orthorectified the photos making each pixel in the image equal to one square millimeter of the deposit. One main use of the overhead photos was to allow us to separate the dry and wet parts of the surface. We added blue dye to the water which nicely contrasts with the brown walnut shells and makes it easier to find the interface between the land and water.

We also measured topography scans with a programmable laser scanner. The scanner provides elevation maps with 1 mm horizontal resolution and sub-mm vertical resolution. Topography scans were taken much less frequently (one per hour of experiment time) than overhead photos because the experiment had to be paused to perform a scan.

2.3 Experimental Runs

We created four separate deltas, varying delta topset slope and base level rise rate. To control the topset slope, the sediment supply was changed to increase or decrease the

ratio of volumetric sediment to water discharges, Q_s/Q_w (Table 1). This meant that the slope was not explicitly controlled, rather it was a natural result of the river sediment

Run Name	Qw (L/s)	Qs (L/s)	Qw/Qs	Slope	Sea Level Rise Rate (mm/hr)
Shallow-Fast	0.1	0.001	100	0.008	5
Shallow-Slow	0.1	0.001	100	0.009	2.5
Steep-Fast	0.1	0.002	50	0.017	5
Steep-Slow	0.05	0.001	50	0.014	2.5

Table 1: Input parameters for the four runs along with the resulting delta top slope.

concentration. Slope and sea level rise rate were chosen because they control the rate at which the islands move in response to base level rise. For example, for a given amount of sea level rise, an island moving up a shallow slope has to move farther laterally than an island moving up a steep slope, to avoid being drowned by the rising water. The rate at which the sea level rises determines how fast the island must retreat up the slope.

2.4 Transgression

The introduction of waves to the delta eroded the shoreface and deposited some of the sediment on the beach, creating a shore-parallel sandbar (Fig. 2). The low area between the delta and this bar became a lagoon as it filled with river water from the land and basin water from the overtopping waves. Areas near the river mouths could not build up a bar as the river eroded bars as soon as they began forming. Once the transgression began, the river mouths were pushed back, and could no longer erode the bars formed by the waves so that a more laterally complete barrier island was formed. This method of

formation follows the theory of barrier island formation first proposed by Hoyt (1967). Hence one primary observation is that transgression tends to create more continuous barriers and wider lagoons than the same wave and river conditions would with constant RSL. The idea that delta morphology relies not just on relative river, wave, and tide power but also on whether it is regressing or transgressing has been suggested before (Boyd, Dalrymple, & Zaitlin, 1992). As the RSL rose, the waves eventually overtopped the barrier islands, beginning overwash and moving the island up the delta slope.

As mentioned above, we controlled total wave energy delivery to the coast by varying wave intermittency. We ran the wave maker in thirty second to one-minute intervals that totaled six minutes per hour, for an intermittency of 10%. Apart from allowing for more precise control of wave input, this allowed us to take overhead photos between wave intervals so that the water level at the shore was not affected by the waves. We used these photos to track the location of both the basinward shoreline and the landward shorelines of the barrier islands over the course of the transgression. To track these two points, we drew a transect from the river source out towards the open water at a specified angle; the two barrier-edge points were defined by the places where the two shorelines intersected this transect (Fig. 2).

After a certain amount of sea level rise, the delta reaches its new equilibrium size, in which the product of the topset area and RSL rise rate balances the sediment input, and the rivers begin to erode the barrier islands. This ends the migration of the island. For each run we chose the transect angle to give us the longest continuous island migration,

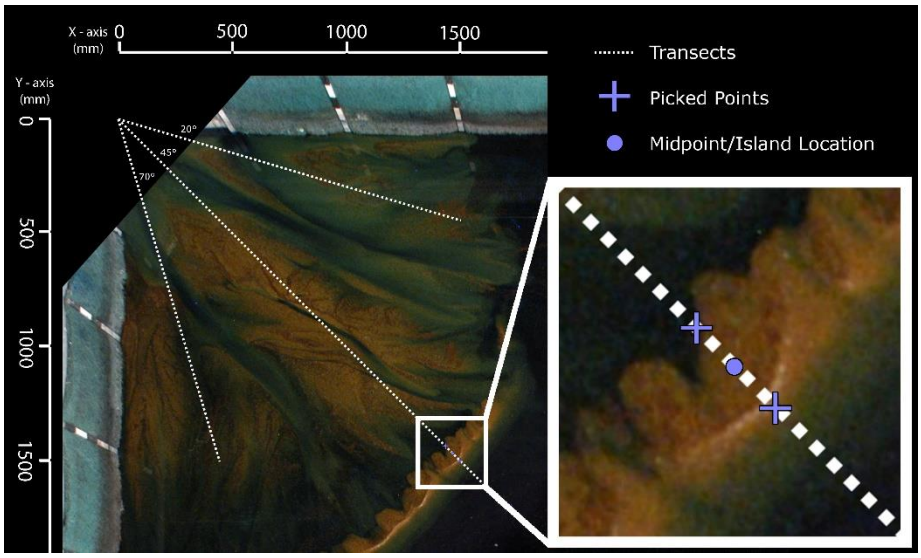

Figure 2: Overhead photo showing a typical experimental barrier and the method used to find the ocean and lagoon shorelines. Example transects for 20°, 45°, and 70° are plotted. The island middle is defined as the midpoint between the two shorelines.

or the section of island that is eroded by the rivers last. The points were manually picked from overhead images taken just after a wave interval. We calculated the distance from the river source to each of these two points. The difference between their distances gave us the width of the island and the midpoint of the two points was called the island middle and was used as the 'true' location of the island. To remove noise we passed the time series of these location points through a low-pass filter calibrated to eliminate signals with a period shorter than 30 min.

An additional point of interest is the location of the delta shoreline as it retreats behind the barriers. To define these complex shorelines we use the Opening-Angle Method (OAM) from J. B. Shaw et al., (2008). The OAM uses a binary land-water image as its input. To retrieve the shoreline of only the delta and not the barrier islands, the islands were manually erased from the land-water images. The method takes the binary

image and defines a convex hull around the land points to divide the image into a delta portion and an open-water portion. For each point in the delta portion, OAM finds the number of swath angles that extend into the open-water. We used the threshold angle of

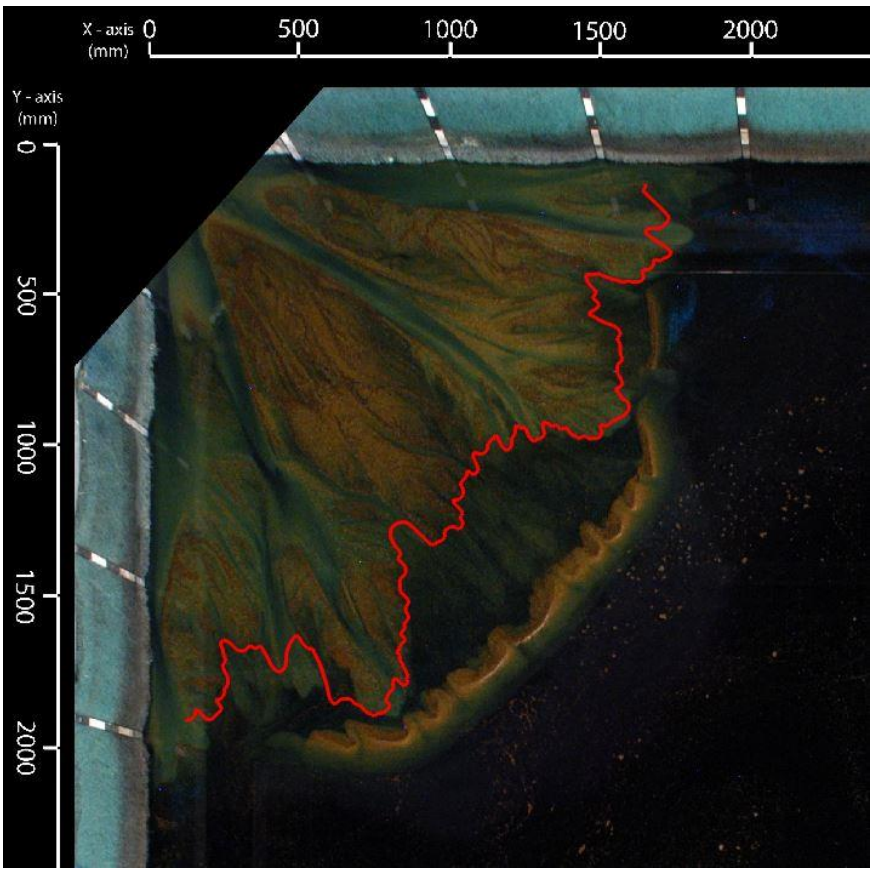

Figure 3 Example of a shoreline defined by the Opening-Angle Method with a threshold value of 45°.

45° for all images, which defines the shoreline as the set of land-water interface points (water points where the interface is not available) with more than 45° of view to open water. An example of the output from this method is shown in Figure 3. The resulting

shoreline was used to find the area of the delta top and the delta radius was defined as the radius of a quarter-circle with an equivalent area.

3 Results

3.1 Barrier Retreat

The experiments successfully created barrier islands and the islands moved upslope as the transgression progressed. Figure 4 shows the position of the island middle

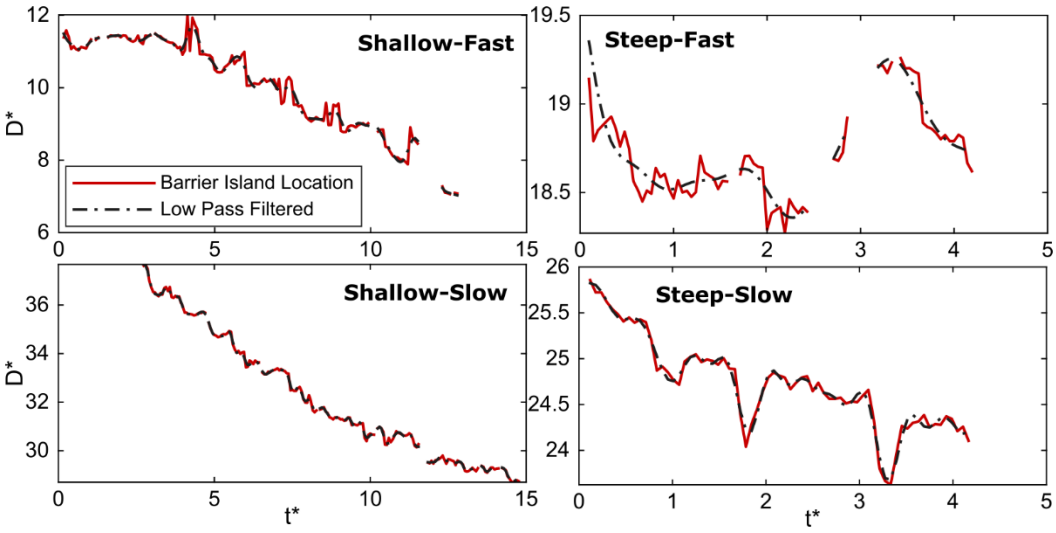

Figure 4: Time series of island midpoint locations for each of the runs (solid), with a 30-min low-pass filter (dashed).

throughout the transgression of the four experiment runs. The non-dimensional distance (D^*) from the delta source is defined as:

$$D^* = \frac{D}{\bar{W}} \qquad (1)$$

Where D is the measured distance from the delta source and $\bar{W}$ is the average barrier island width for that experiment run. Non-dimensional time t^* is defined as:

$$t^* = t * \frac{\dot{H}}{A} \qquad (2)$$

Where *t* is time, $\dot{H}$ is the base level rise rate, and *A* is the open-water wave amplitude.

The graphs show the same overall trend of ongoing transgression due to the rising RSL. The overall retreat rate decreases with time as the deltas approach their new equilibrium size under constant sea level rise rate. However, the transgression is clearly not steady, and includes intervals of transient regression or steps. Once an island moves upslope, it remains in place for a period of time or even moves back downslope before once again moving upslope. The overall variability in shoreline migration rate clearly changes between the runs.

As the barrier island retreats, the delta shoreline retreats behind it. As mentioned previously, the barrier island begins as a ridge along the delta edge and becomes detached from the delta as the low area behind the island is flooded (Hoyt, 1967). Figure 5 is the plot of the two lagoon shorelines with time along with the simple retreat path. Simple retreat is the path a delta shoreline takes as it approaches its new equilibrium size. The path is found from solving the mass-balance equation:

$$\frac{dR}{dt} = \frac{\dot{H}}{S} - \frac{4Q_s}{SR^2\pi} \qquad (3)$$

Where *R* is the delta radius, *S* is the delta-plain slope, $\dot{H}$ is the base level rise rate, and Q_s is the sediment supply. The $\dot{H}$ term is the amount of transgression given an amount of RSL rise in the absence of deposition, and the second term is the progradation caused by vertical accretion of the sediment supply on a quarter circle delta-plain of a given radius. The difference between these two terms is the is the total change is shoreline location

caused by the balance between these two effects. The result is that when a delta radius is much larger than its equilibrium size, the amount of change in shoreline location is large; as transgression continues, the delta approaches its equilibrium size asymptotically. Note also that the mass balance in equation (3) assumes that all delivered sediment is retained behind the shoreline, i.e. no loss to the offshore region.

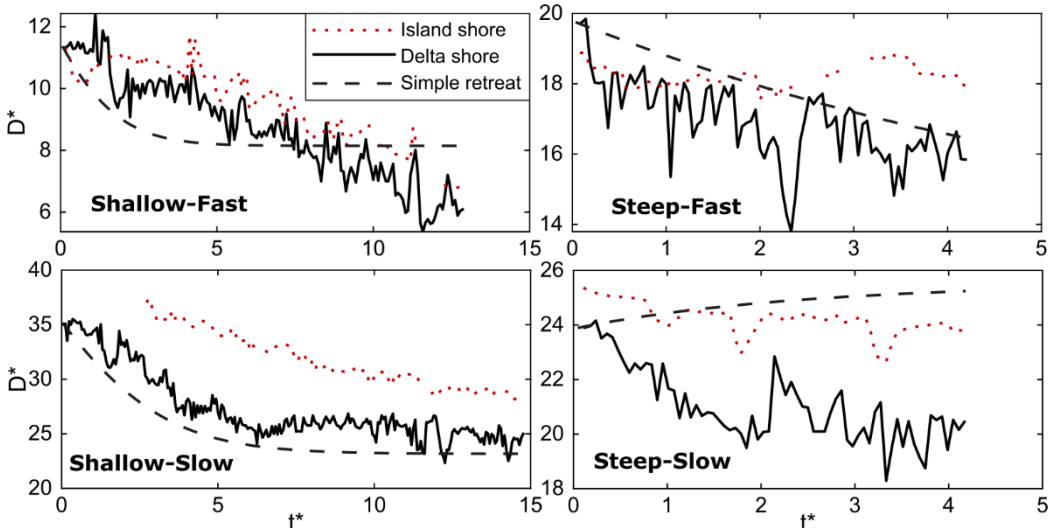

Figure 5*: Time series of the two lagoon shores through time with the simple retreat path. Non-dimensional variables follow equations 1 and 2.*

The plots show that the two shorelines begin close together and separate throughout the run. The simple retreat path for the Steep-Slow case shows that the delta shoreline should prograde instead of transgressing, but the measured shoreline shows retreat. This could be explained by sediment washing through the system and not being deposited on the delta which would effectively reduce the sediment supply to the delta.

We calculated island migration velocities as the first derivative of the low-pass filtered location time series. These velocities are plotted in Figure 6 along with the

measured mean velocity, the simple retreat velocity from equation (3), and the geometric drowning velocity (the transgression velocity from equation (3) with no sediment supply). Non-dimensional velocities (V^*) are defined as:

$$V^* = \frac{V}{\dot{H}} \qquad (5)$$

With V as the measured velocity and $\dot{H}$ the base level rise rate.

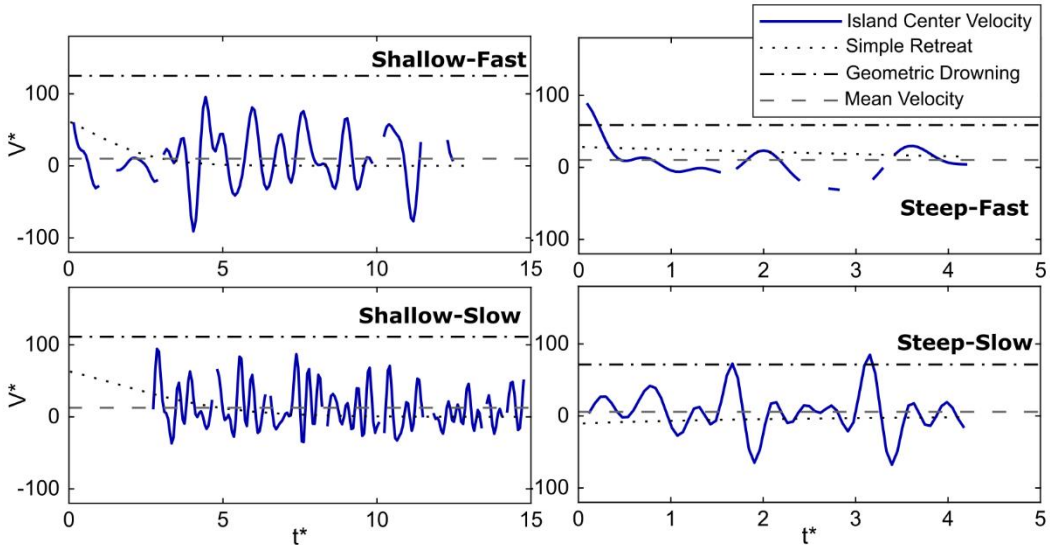

Figure 6*: Plots of the velocity of the islands through time. Velocities were found by taking the first derivative of the low pass filtered location time series. Also plotted are the simple retreat velocity, the geometric drowning velocity, and the mean velocity.*

All the measured island retreat rates are closer to the simple retreat rate than the geometric drowning rate. Island width was non-constant as well over the course of the transgression (figure 7). Non-dimensional width (W^*) is defined as:

$$W^* = \frac{WS}{A} \qquad (6)$$

Where *W* is the measured barrier island width, *S* is the delta-plain slope, and *A* is the open-water wave amplitude.

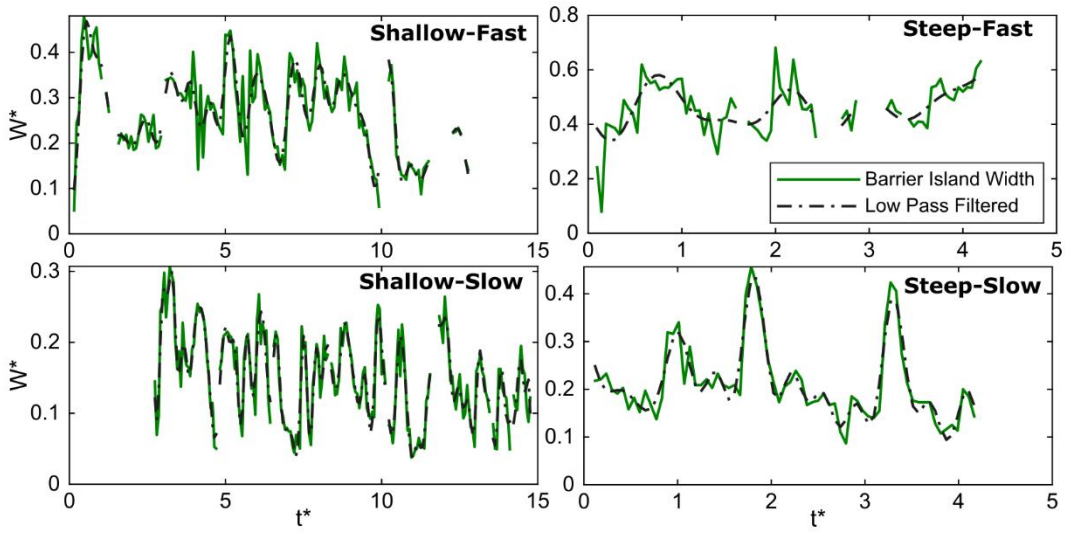

Figure 7: Time series of island width for each run (solid) with a 30-min low pass filter (dashed).

4 Discussion

4.1 Island Retreat Rates

The location data for the islands moving over a delta top show clearly that the islands do not move at a constant velocity. The overall trend is a transgression, as expected. There are intervals where the island location moves opposite to this trend for short periods of time. This behavior can be explained by the way islands are tracked; the island location is the midpoint between the ocean shore and the lagoon shore. The barrier island has different slopes near these two points which means that for a single increment of sea level rise, the two shores can retreat different amounts. If the lagoon beach has a shallower slope than the ocean beach, the lagoon beach will shrink at a faster rate than the ocean

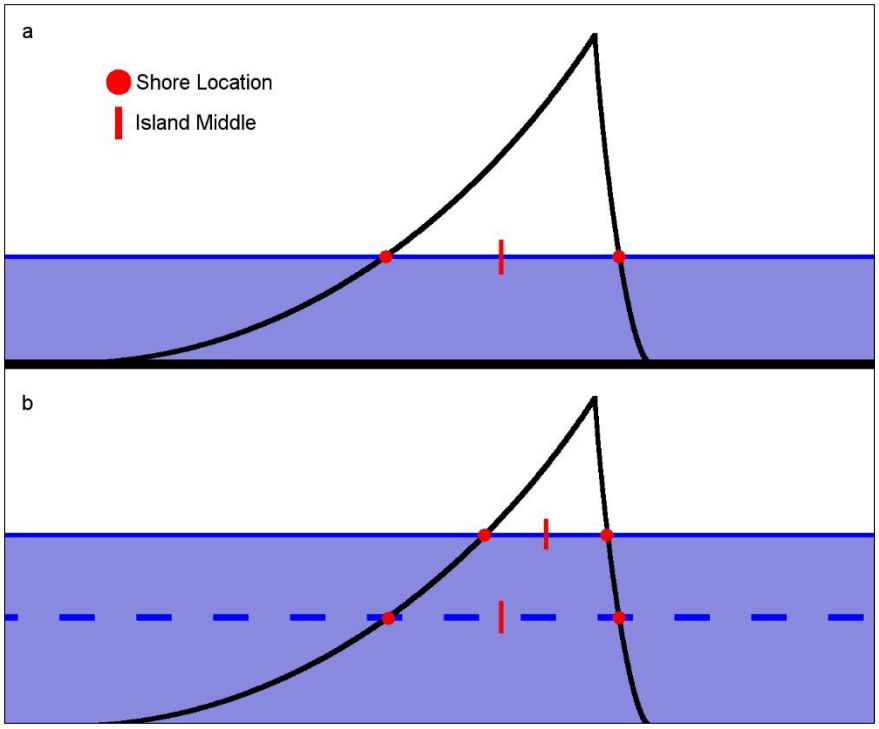

Figure 8: Schematic showing how movement in the "wrong" direction is possible. a) A wide island after overwash has taken place and backfilling has formed a new ridge. b) After an amount of sea level rise the two shorelines moved different amounts, moving the island middle.

side if they are both experiencing the same sea level rise. This causes the midpoint of the two shorelines to move oceanward (Fig. 8). Figure 9 shows this behavior in the location time series of the two shorelines, instead of their midpoint. These time series show that the landward shore is responsible for most of the basinward movement. Both time series show non-constant movement, but the variability is much more pronounced in the landward shoreline.

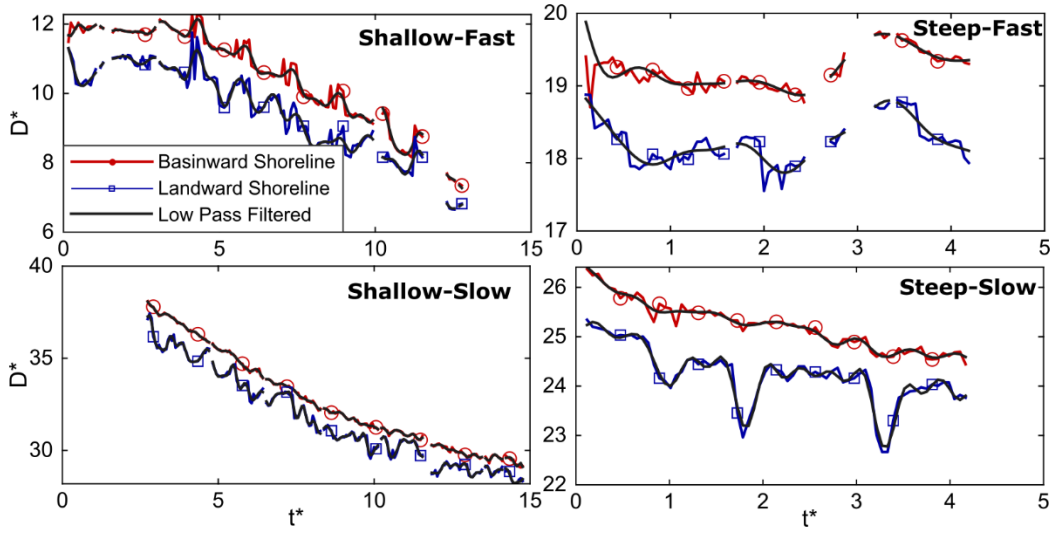

Figure 6: Time series of the basinward and landward shorelines along with a 30-min low pass filter.

This movement in the "wrong" direction is always followed by a step back in the expected direction, overall transgression. It is also typically associated with a widening of the island (Fig. 7). This means that the periods of highest transgression velocity of the island should correlate with a widening of the barrier. To test this idea, we attempted to use the island width to predict the velocity (V_W) using a simple equation:

$$V_W = \frac{dW}{dt}\left(\frac{W}{A\bar{W}}\right) \qquad (7)$$

Where W is the 30-min lowpass filtered island width, t is time, $\bar{W}$ is the average island width for that run, and A is the open-water wave amplitude. Fluctuations in the location of the landward shoreline affect both the width and island center velocity. We will try to predict the basinward shoreline velocity because it is not obviously affected by changes in width, as the landward shoreline and island middle are. The predictions are plotted against the measured values in Figure 10; the generally good correlation suggests a

significant relation between island width and migration rate, which we explore further in the next section.

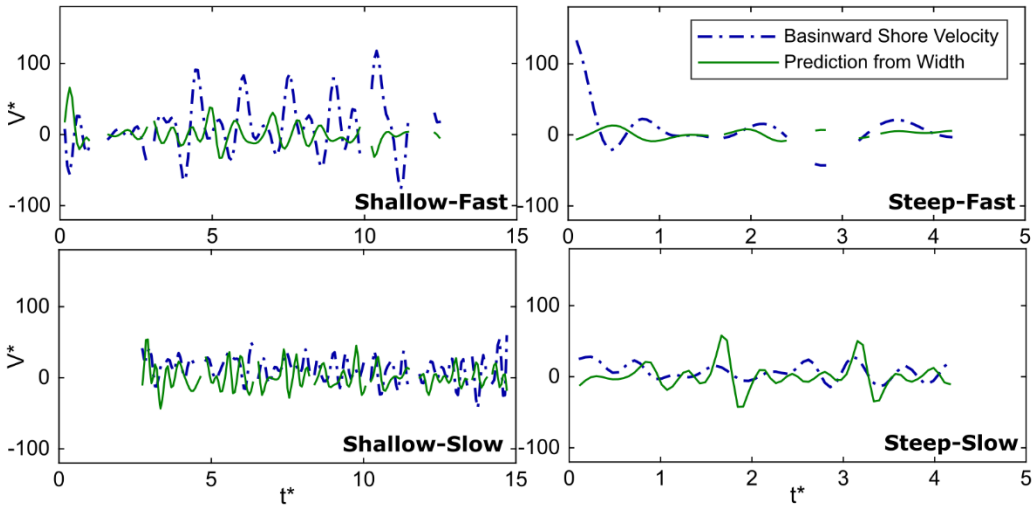

Figure 7: Time series of the basinward shoreline velocity and the prediction from the low pass filtered island.

4.2 Variable Retreat Mechanism

Having established a connection between island width and retreat rate, we next use the topography scans understand how island height changes might figure into retreat dynamics. Because the time resolution of the topography scans is much lower than the overhead photos, no scan was taken exactly when the measured width of the island was at its maximum or minimum. Fortunately, the variation in width is not just time dependent; it varies over space as well. In each scan there are parts of the islands that are narrower or wider than average. To compare the heights of the wide and narrow islands, representative parts of the island were chosen from the scans. These representative areas were chosen based on their similarity to the maximum and minimum widths measured along the transect for the time series.

These profiles show that variation in island width is related to variation in island height (Fig. 11).

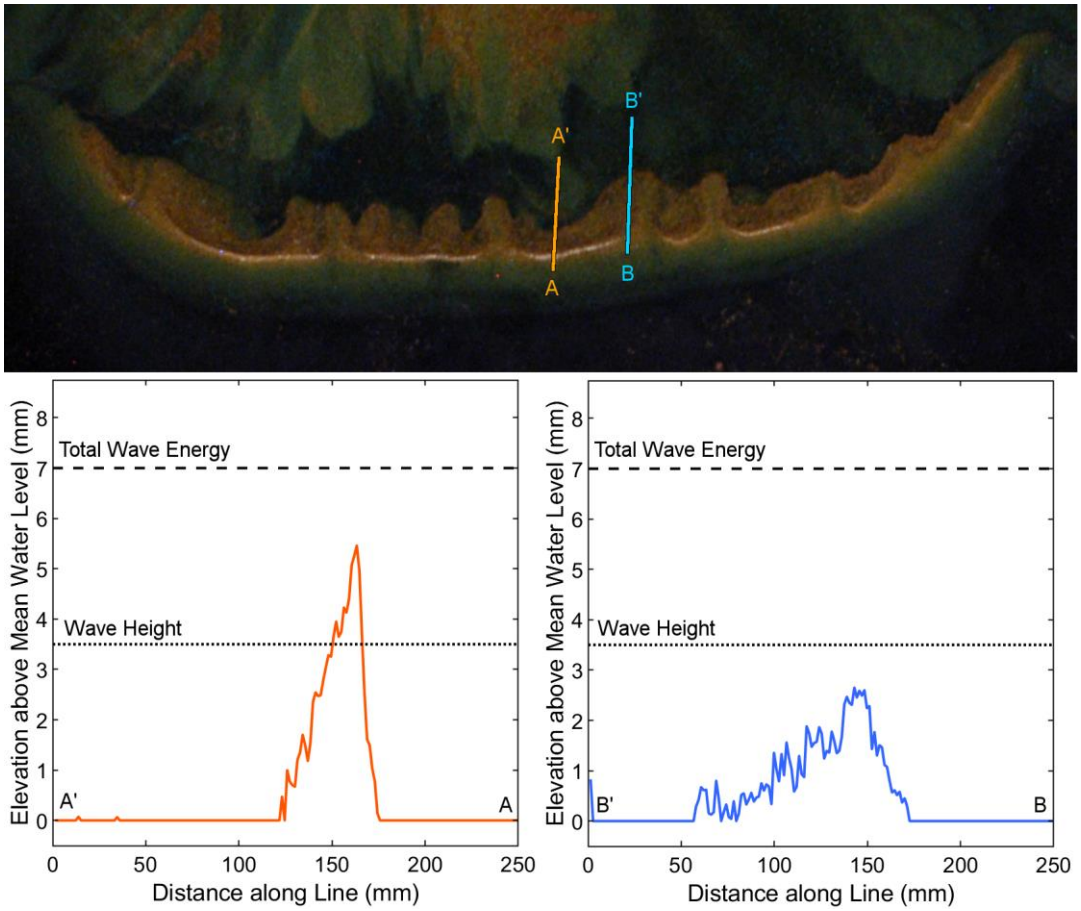

Figure 11: Two cross sections across a thin and wide portion of the island. In cross section A the island width is low but the island height is large and in cross section B, the opposite is true, the width is large but the height is small.

The narrow parts of the island have a tall ridge that is absent in the wider sections. The ridge of the island featured in Figure 11 is 5.5mm tall, 2mm taller than the open-water wave height. Waves exchange energy between kinetic and potential as they propagate and according to the equipartition theorem, those two energies are equivalent. As a wave approaches the shoreline, it is slowed and some of its kinetic energy is

transferred to potential energy, increasing the wave height. The limit of this is that the wave could reach twice its deep-water height if (unrealistically) it transferred all its kinetic energy without loss. While we could not measure the exact heights of breaking waves in these experiments, it is likely that the wave lost significant energy during shoaling, meaning that the breaking wave did not approach twice the height of the deep-water wave. This is reflected in the fact that the island ridge is between the height of the deep-water wave and twice this value.

Matching these profiles with the relationship between island width and velocity means that the islands move landward during a transition from having a ridge to not having a ridge. One explanation of that behavior is overwash. If waves overtop the island they can erode the ridge and then deposit that sediment behind the island. To check this idea, close-up photos and videos were taken of the islands while waves were breaking on them. These photos and videos reveal that overwash is the main driver of island retreat agreeing with previous field and numerical studies (Leatherman, 1979; Lorenzo-Trueba & Ashton, 2010; Moore et al., 2010). Locally, the islands go through a cycle of having a ridge, overwash eroding that ridge, and then the ridge forming again.

These transitions are governed by a tendency for larger waves to erode sediment and smaller waves to deposit. The waves in the open water of the experiment are all the same size, but how they interact with the barrier island changes depending on what stage of the morphology cycle the island is in. An island with a tall ridge can block much of a wave when it breaks but as the sea level rises, the ridge becomes relatively smaller and

more of the wave can overtop the island. The relative size of the wave with respect to the island keeps increasing as the RSL rises until the waves can overtop the island sufficiently to begin to erode the ridge. These relatively larger waves carry that eroded sediment to the back of the island, all the while losing energy to friction. As they lose energy and spread, the waves become smaller and can no longer carry the eroded sediment; the wave deposits sediment behind the island. This process removes the ridge and widens the island, which matches the transition seen in the island profiles.

Figure 12 shows the process of a relatively small wave becoming larger as the sea level increases.

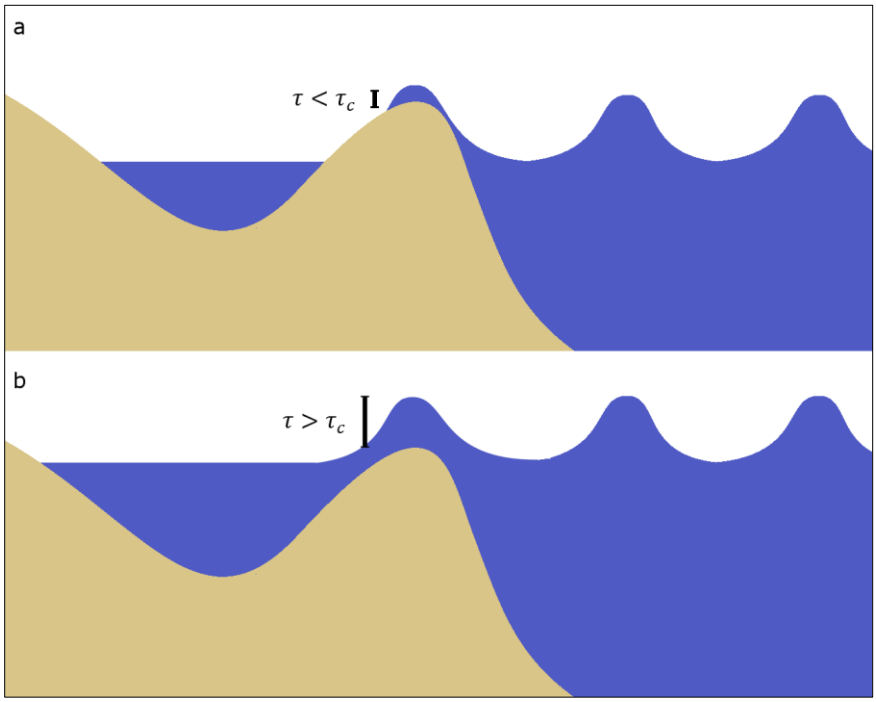

Figure 12: a) Snapshot of the wave environment soon after a ridge is formed where the ridge and waves are on the same scale. The waves cannot push enough water over the top of the ridge to surpass the shear stress needed to erode sediment. b) The same ridge after some amount of sea level rise. Now the wave are larger compared to the island and able to push enough water over the top of the island to surpass the critical shear stress and erode sediment.

With sea level increasing steadily, each wave can push more water over the crest of the ridge than the last one. Eventually, one wave pushes enough water over the ridge that the critical shear stress is surpassed, and some sediment is picked up by the pulse of water and carried to the back of the island. As the next wave crashes against the ridge, it has an easier time sending water over the island because the previous wave shortened the ridge by eroding it. This creates a positive feedback loop where each subsequent wave has an easier time eroding the ridge than the previous wave.

Eventually, the waves no longer cross the entire width of the island, allowing deposition and ridge growth to begin again. Figure 13 shows this process in action. An

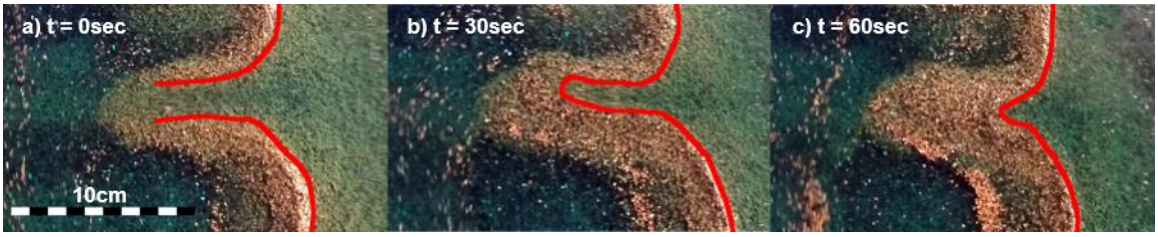

Figure 13: Progression of an overwash channel to a ridge. All three photos are taken at the time of maximum swash of a wave. a) An open overwash channel that is approaching the maximum length that the waves can transport sediment across. b) The same overwash channel once sediment was deposited in the outlet, blocking future waves. c) The former overwash channel after the majority of it has been filled in.

open channel that allows waves to travel through it eventually becomes so long that waves can no longer transport sediment effectively all the way through the channel. The wave drops its sediment at the end of the channel, blocking future pulses of water from continuing through. Each subsequent wave drops it sediment, eventually closing the once-open channel. From the experiments, the amount of time needed for this process is variable; some channels filled quickly after the initial “plug” was deposited, while other channels branched around the deposited sediment, opening new paths to the lagoon.

This cycling was seen in all four experiments, but the details changed slightly between runs. We can look at the frequency spectrum of the location time series to better understand how the timing of the overwash cycle changes between experiments. We would expect the experiments with a slower sea level rise rate to have longer period cycles as the rising sea sets the timing for the waves to overtop the islands and move them.

Figure 14 shows standard squared-FFT spectra of island location for the four experimental runs, with the significant peaks (p = 0.05) labeled with their period in t* units. We used surrogate data testing to find the significance of peaks in the spectra. Surrogate data testing is a Monte Carlo method where we create multiple artificial time series by randomly shuffling our input time series. We then find the mean and standard deviation of the spectra of the artificial time series to determine the confidence interval.

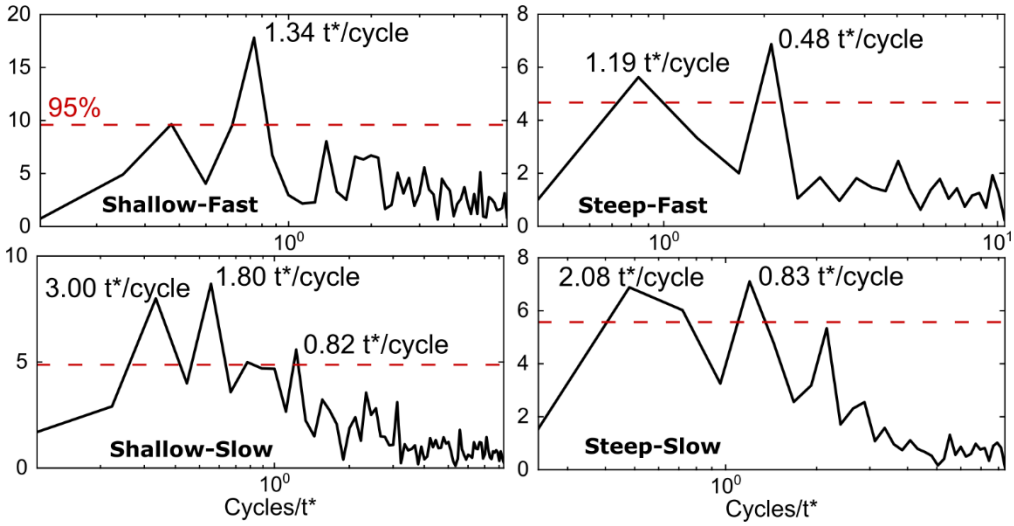

Figure 14: Squared-FFT frequency spectra of the four location time series with the 95% confidence interval. Significant peaks are labeled with their corresponding periods.

To further illustrate the significance of the peaks in the observed data, Figure 15 shows the probability density functions (PDF) of both the observed spectra and the shuffled time series spectra. While both curves are right skewed, the observed PDFs show a second peak at higher values that is absent from the shuffled time series case.

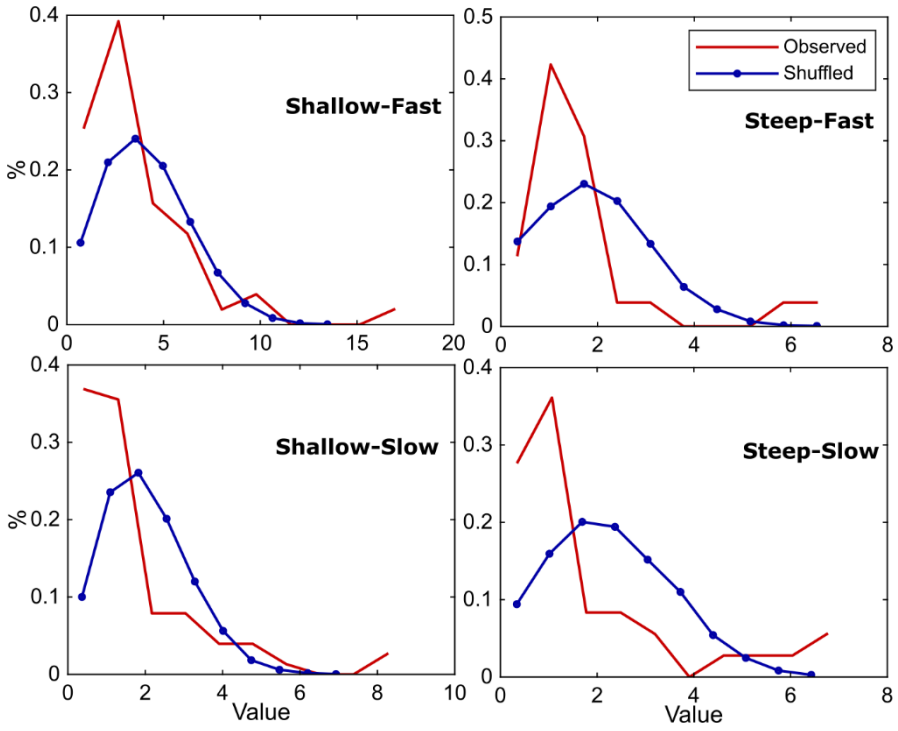

Figure 15: Probability density functions of the observed spectra and the shuffled time series spectra. Both curves are right skewed, but the observed PDFs show a second peak at higher values.

By looking at the location time series for reference, we estimate that the period of the process we are interested in is near 1 to 2 t^* units. For the high sea level rise rate experiments, there are peaks at periods of 1.19 and 1.34 t^* units and for the low sea level rise rates there are peaks at 0.82 and 0.83 t^* units. Our method of using base level rise rate to non-dimensionalize time did not align the peaks of all the runs. Between the low

base level rise rate and the high rise rate experiments, the rise rate was doubled and if the cycle period also doubled, the peaks would align in non-dimensional space.

This did not occur and can be explained by looking at what specifically sea level rise rate controls. The overwash cycle can be divided into two halves; one where waves overtop the island to begin overwash and another where the overwash fan is back-filled once it becomes too long. These two parts of the cycle are controlled by different mechanisms in these experiments; only the amount of time between ridge formation and overwash is dependent on the rate of sea level rise. Once an overwash fan is formed, the rate of sea level rise has little effect on how fast it is filled in. In our case, when we doubled the sea level rise rate, we approximately halved the time it takes for one only part of the cycle.

5 Conclusions

Using physical experiments, we studied barrier island behavior at high time resolution under controlled, steady RSL rise, focusing on time series of barrier-island location. The main findings are:

1. Experimental barrier islands do not retreat at a constant rate under constant sea level rise and a constant wave environment. This autogenic stepping supports the idea of discontinuous retreat suggested by Lorenzo-Trueba and Ashton, (2010).
2. The non-constant retreat rate is controlled by a cycling of morphologies between a ridged island and a non-ridged island. Overwash that erodes the ridge is the

mechanism for upslope retreat; then back filling of the overwash fan creates a new ridge and the cycle restarts.

3. Increased sea level rise rates increase the frequency of retreat events (steps). Doubling the rise rate does not double the frequency of retreat events because the rise rate controls only the overwash frequency, not the rate of ridge growth.

3 Conclusion

The physical experiments presented here shows how complex retreat behavior and can arise from simple environmental settings. The main findings of this thesis are:

1. Experimental barrier islands do not retreat at a constant rate under constant sea level rise and a constant wave environment. This autogenic stepping supports the idea of discontinuous retreat suggested by Lorenzo-Trueba and Ashton, (2010).
2. The non-constant retreat rate is controlled by a cycling of morphologies between a ridged island and a non-ridged island. Overwash that erodes the ridge is the mechanism for upslope retreat; then back filling of the overwash fan creates a new ridge and the cycle restarts.
3. Increased sea level rise rates increase the frequency of retreat events (steps). Doubling the rise rate does not double the frequency of retreat events because the rise rate controls only the overwash frequency, not the rate of ridge growth.

Simple experiments can reveal a lot about a system. Overwash is a key aspect to an island's lifecycle; if an island is not able to retreat upslope it will likely drown to RSL rise. The addition of tides and storm events like we see in the field would make these results more analogous to islands in the field, but the simplicity of these experiments shows that this behavior is an intrinsic aspect to barrier island systems.

Future Work

While this work successfully produced barrier islands and recorded their behavior, much is still unknown about these systems. Throughout these runs, overwash was one of the dominant behaviors that islands exhibited. Understanding the process of overwash in more detail will help us apply this work more accurately in the field. For example, what controls the width of an overwash fan? There were times in these experiments where entire islands transitioned to overwash and other times where just a small part would erode into an overwash fan. When islands in the field are hit by storm events will the entire island experience overwash or just a small section?

Predicting where overwash fans will form in the future would help with barrier island restoration and protecting human infrastructure. It may be possible to better predict where these fans will be created by treating them as compensational; where new overwash fans avoid areas with previous fans. This idea is expanded on in the appendices.

Looking to the field, there is a new variable that could have massive impacts on the behavior of islands: tides. Previous work done by Lentsch, Finotello, and Paola, (2018) found that subjecting an experimental delta to tides increases channel stability by flushing out sediments accumulating in channels. The inclusion of tides could change the overwash cycle completely as tides could keep overwash channels open for longer by removing the “plug” of sediment that stops waves from moving completely through the channel. We discovered that the rate of sea level rise is responsible for the frequency of

one half of the overwash cycle, overwash initiation and ridge erosion. It is possible that tides are partly responsible for the frequency of ridge formation where stronger tides inhibit ridge formation and increase the period of the cycle.

References Cited

Beets, D. J., & Van Der Spek, A. J. F. (2000). The Holocene evolution of the barrier and the back-barrier basins of Belgium and the Netherlands as a function of late Weichselian morphology, relative sea-level rise and sediment supply. *Geologie En Mijnbouw/Netherlands Journal of Geosciences*, *79*(1), 3–16. https://doi.org/10.1017/S0016774600021533

Boyd, R., Dalrymple, R., & Zaitlin, B. A. (1992). Classification of clastic coastal depositional environments. *Sedimentary Geology*, *80*(3–4), 139–150.

Burger, J., & Lesser, F. (1978). Selection of Colony Sites and Nest Sites By Common Terns Sterna Hirundo in Ocean County, New Jersey. *Ibis*, *120*(4), 433–449. https://doi.org/10.1111/j.1474-919X.1978.tb06810.x

Ciarletta, D. J., Shawler, J. L., Tenebruso, C., Hein, C. J., & Lorenzo-Trueba, J. (2019). Reconstructing Coastal Sediment Budgets from Beach-and Foredune-Ridge Morphology: A Coupled Field and Modeling Approach. *Journal of Geophysical Research: Earth Surface*, 0–2. https://doi.org/10.1029/2018JF004908

Donnelly, J. P., & Woodruff, J. D. (2007). Intense hurricane activity over the past 5,000 years controlled by El Niño and the West African monsoon. *Nature*, *447*(7143), 465–468. https://doi.org/10.1038/nature05834

Downing, S. (2013). *Hidden History of the Outer Banks*. Arcadia Publishing.

Emanuel, K. A. (2013). Downscaling CMIP5 climate models shows increased tropical cyclone activity over the 21st century. *Proceedings of the National Academy of*

Sciences, *110*(30), 12219–12224. https://doi.org/10.1073/pnas.1301293110

Houser, C. (2012). Feedback between ridge and swale bathymetry and barrier island storm response and transgression. *Geomorphology*, *173–174*, 1–16. https://doi.org/10.1016/j.geomorph.2012.05.021

Hoyt, J. H. (1967). Barrier island formation. *Geological Society of America Bulletin*, *78*(9), 1125–1136. https://doi.org/10.1130/0016-7606(1967)78

Leatherman, S. P. (1979). Migration of Assateague Island, Maryland, by inlet and overwash processes. *Geology*, *7*(2), 104–107.

Leatherman, S. P. (1983). Barrier dynamics and landward migration with Holocene sea-level rise. *Nature*, *301*(5899), 415–417. https://doi.org/10.1038/301415a0

Lentsch, N., Finotello, A., & Paola, C. (2018). Reduction of deltaic channel mobility by tidal action under rising relative sea level. *Geology*, *46*(7), 599–602. https://doi.org/10.1130/G45087.1

Lorenzo-Trueba, J., & Ashton, A. D. (2010). Rollover, drowning, and discontinuous retreat: Distinct modes of barrier response to sea-level rise arising from a simple morphodynamic model. *Journal of Geophysical Research: Earth Surface*, *119*(4), 779–801. https://doi.org/10.1002/2013JF002941

Losada, I. J., Reguero, B. G., Losada, I. J., & Méndez, F. J. (2019). A recent increase in global wave power as a consequence of oceanic warming. *Nature Communications*, *10*(1), 205. https://doi.org/10.1038/s41467-018-08066-0

Moore, L. J., List, J. H., Williams, S. J., & Stolper, D. (2010). Complexities in barrier

island response to sea level rise: Insights from numerical model experiments, North Carolina Outer Banks. *Journal of Geophysical Research*, *115*(F3), F03004. https://doi.org/10.1029/2009JF001299

NPS, N. P. S. (2017). 2016 National Park Visitor Spending Effects Economic Contributions to Local Communities , States ,.

Sanders, J. E., & Kumar, N. (1975). Evidence of shoreface retreat and in-place "Drowning" during holocene submergence of barriers, shelf off Fire Island, New York. *Bulletin of the Geological Society of America*, *86*(1), 65–76. https://doi.org/10.1130/0016-7606(1975)86<65:EOSRAI>2.0.CO;2

Shaw, J. B., Wolinsky, M. A., Paola, C., & Voller, V. R. (2008). An image-based method for shoreline mapping on complex coasts. *Geophysical Research Letters*, *35*(12), 1–5. https://doi.org/10.1029/2008GL033963

Shaw, J., You, Y., Mohrig, D., & Kocurek, G. (2014). Tracking hurricane-generated storm surge with washover fan stratigraphy. *Geology*, *43*(2), 127–130. https://doi.org/10.1130/G36460.1

Stapor, F. W., Mathews, T. D., Lindfors-kearns, F. E., Journal, S., Summer, N., Stapor, F. W., … Lindfors-kearns, F. E. (1991). Barrier-island progradation and Holocene sea-level history in southwest Florida. *Journal of Coastal Research*, *7*(3), 815–838.

Stick, D. (2015). *The Outer Banks of North Carolina, 1584-1958*. UNC Press Books.

Stutz, M. L., & Pilkey, O. H. (2011). Open-ocean barrier islands: Global influence of climatic, oceanographic, and depositional settings. *Journal of Coastal Research*,

27(2), 207–222. https://doi.org/10.2112/09-1190.1

Swift, D. J. P. (1975). Barrier-island genesis: evidence from the central atlantic shelf, eastern U.S.A. *Sedimentary Geology*, *14*(1), 1–43. https://doi.org/10.1016/0037-0738(75)90015-9

White, R. (2008). A Commemoration and a Historical Mediation. *Journal of American History*, *94*(4), 1073–1081. https://doi.org/10.2307/25095320

Wright Memorial Bridge. (1932, November 18). *The Daily Advance*.

Wright, W., McFarland, M. W., Chanute, O., & Wright, O. (1953). The papers of Wilbur and Orville Wright, including the Chanute-Wright letters and other papers of Octave Chanute. New York: McGraw-Hill. Retrieved from file://catalog.hathitrust.org/Record/001114607

Appendix A

Compensational Overwash Fans

A simple observation from these experiments is that entire islands were able to retreat inland to keep up with sea level rise. What is interesting is that a relatively small feature, an overwash fan, can lead to transport of the entire length of an island up the

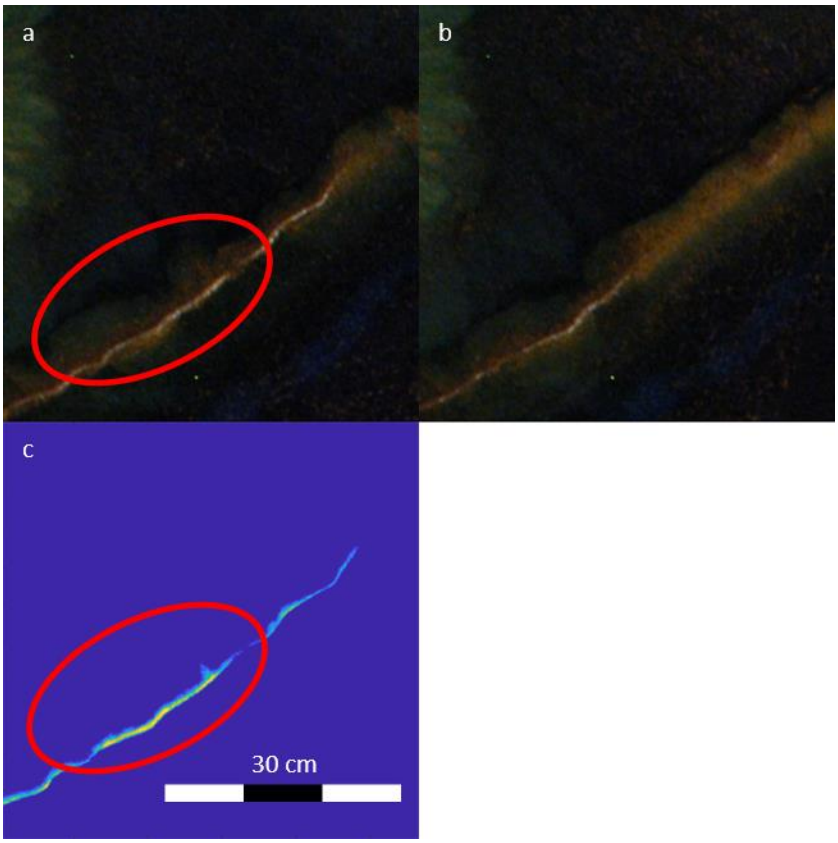

Figure 8: a) Section of island with a ridge along the majority of it. The circled section in the lower left has been submerged while the upper right part of the island is missing these submerged features. This suggests that the circled portion of the island underwent overwash more recently than the upper part. b) the same portion of island after 30 seconds of waves. The lower left portion is largely unchanged but the upper right section has transitioned from ridge-bearing to overwash. c) An elevation map of the island seen in "a." The colorbar is modified to focus on only the ridge height along the island. The circled portion has a higher ridge than the upper right section of the island.

delta slope. The overwash fans can do this because they are compensational; new overwash fans tend to avoid the locations of recent previous fans. Figure 15 gives an example of overwash favoring areas not occupied by recent prior overwash events.

For example, an overhead photo (Figure 15) taken just after a topography scan, shows an island with a ridge along most of it. In the bottom left part of the island there are visible submerged overwash fans; those fans are missing elsewhere in the island. Matching up the topography scan with the overhead photo shows that the area with the submerged fans has a higher ridge. An image from just after the next set of waves reveals that the area with no submerged overwash fans and a lower ridge transitioned to an overwash fan. This process eventually allows entire islands to retreat more or less coherently.

Time Series Data

Below are four tables, each containing the data used to create the time series plots (Figs. 4, 5, 6, 7, 9).

Run: Shallow Fast

Time (HH:MM:SS)	Landward Shoreline Distance (mm)	Basinward Shoreline Distance (mm)	Island Middle Distance (mm)	Island Width (mm)	Island Middle Velocity (mm/min)	Delta Radius (mm)
0:00:00	1328.02	1350.63	1339.32	22.60	NaN	1332.19
0:03:20	1308.60	1415.25	1361.93	106.65	4.89	1337.43
0:06:40	1282.81	1399.02	1340.91	116.21	3.23	1351.01
0:10:00	1208.31	1394.24	1301.28	185.93	2.21	1326.33
0:13:20	1205.13	1415.25	1310.19	210.13	1.84	1328.84
0:16:40	1203.54	1397.43	1300.48	193.89	1.68	1352.08
0:20:00	1213.09	1381.51	1297.30	168.42	1.22	1327.89
0:23:20	1221.37	1394.24	1307.80	172.88	0.26	1346.96
0:26:40	1209.91	1402.52	1306.21	192.61	-1.00	1311.68
0:30:00	1203.54	1402.52	1303.03	198.98	-2.08	1309.59
0:33:20	1236.01	1400.93	1318.47	164.92	-2.58	1325.00
0:36:40	1257.02	1407.30	1332.16	150.27	-2.39	1315.78
0:40:00	NaN	NaN	NaN	NaN	NaN	1461.21
0:43:20	1263.39	1399.02	1331.20	135.63	NaN	1281.55
0:46:40	1279.63	1397.43	1338.53	117.80	-0.43	1267.25
0:50:00	NaN	NaN	NaN	NaN	NaN	1396.17
0:53:20	NaN	NaN	NaN	NaN	NaN	1356.76
0:56:40	NaN	NaN	NaN	NaN	NaN	1371.11
1:00:00	1295.87	1383.10	1339.48	87.23	NaN	1226.69
1:03:20	1297.46	1394.24	1345.85	96.78	-0.51	1173.17
1:06:40	1299.05	1389.47	1344.26	90.42	-0.47	1125.32
1:10:00	1295.55	1391.06	1343.30	95.51	-0.30	1102.61
1:13:20	1305.42	1387.87	1346.65	82.46	-0.01	1138.38
1:16:40	1292.36	1386.28	1339.32	93.92	0.35	1141.10
1:20:00	1305.42	1386.28	1345.85	80.87	0.68	1166.10
1:23:20	1303.82	1386.28	1345.05	82.46	0.90	1247.37
1:26:40	1286.00	1381.51	1333.75	95.51	0.95	1066.82
1:30:00	1271.35	1386.28	1328.82	114.93	0.85	1213.20
1:33:20	1268.17	1381.51	1324.84	113.34	0.67	1167.06
1:36:40	1276.44	1383.10	1329.77	106.65	0.48	1189.03
1:40:00	1300.64	1389.47	1345.05	88.83	0.22	1138.38
1:43:20	1272.94	1374.82	1323.88	101.88	-0.17	1193.55
1:46:40	1260.21	1374.82	1317.51	114.61	-0.74	1156.93

1:50:00	1303.82	1386.28	1345.05	82.46	-1.39	1197.72
1:53:20	1302.23	1386.28	1344.26	84.05	-1.81	1207.87
1:56:40	1299.05	1392.65	1345.85	93.60	-1.71	1198.64
2:00:00	NaN	NaN	NaN	NaN	NaN	1147.89
2:03:20	1276.98	1425.38	1351.18	148.40	NaN	1184.32
2:06:40	1268.84	1418.22	1343.53	149.38	1.42	1213.29
2:10:00	1267.54	1418.22	1342.88	150.68	1.95	1202.63
2:13:20	1261.68	1410.09	1335.89	148.40	1.65	1203.69
2:16:40	1259.41	1400.32	1329.86	140.92	0.87	1143.57
2:20:00	1257.13	1392.19	1324.66	135.06	0.33	1224.41
2:23:20	1254.52	1389.91	1322.22	135.38	0.66	1176.27
2:26:40	1255.83	1387.31	1321.57	131.48	1.86	1124.18
2:30:00	1250.94	1379.17	1315.06	128.22	3.11	1158.77
2:33:20	1232.07	1376.89	1304.48	144.82	3.20	1190.05
2:36:40	1247.36	1368.43	1307.90	121.06	1.35	1191.28
2:40:00	1195.29	1370.71	1283.00	175.41	-2.12	1161.23
2:43:20	1227.19	1368.43	1297.81	141.24	-5.74	1222.60
2:46:40	1381.45	1443.28	1412.36	61.83	-7.57	1116.92
2:50:00	1223.93	1367.13	1295.53	143.19	-6.34	1252.25
2:53:20	1366.15	1439.70	1402.93	73.55	-2.30	1219.46
2:56:40	1320.91	1440.68	1380.80	119.76	2.80	1157.39
3:00:00	1298.46	1431.24	1364.85	132.78	6.72	1095.11
3:03:20	1224.91	1344.67	1284.79	119.76	7.96	1130.35
3:06:40	1221.33	1346.95	1284.14	125.62	6.59	1154.05
3:10:00	1224.91	1343.37	1284.14	118.46	4.02	1125.12
3:13:20	1228.49	1335.23	1281.86	106.75	2.06	1116.48
3:16:40	1230.77	1331.65	1281.21	100.89	1.69	1071.03
3:20:00	1224.91	1320.91	1272.91	96.01	2.62	1106.81
3:23:20	1138.34	1330.35	1234.35	192.01	3.68	1076.75
3:26:40	1131.18	1322.22	1226.70	191.04	3.70	1053.48
3:30:00	1127.60	1323.52	1225.56	195.92	2.35	1105.28
3:33:20	1137.37	1316.36	1226.86	178.99	0.19	1092.74
3:36:40	1171.54	1312.78	1242.16	141.24	-1.86	1021.27
3:40:00	1187.16	1309.20	1248.18	122.04	-3.10	970.82
3:43:20	1211.89	1300.74	1256.31	88.85	-3.42	1092.66
3:46:40	1204.73	1356.71	1280.72	151.98	-3.09	981.48
3:50:00	1208.31	1297.16	1252.73	88.85	-2.31	1027.96
3:53:20	1235.65	1292.60	1264.13	56.95	-1.02	1118.26
3:56:40	1177.39	1354.11	1265.75	176.72	0.89	1145.47

4:00:00	1219.05	1345.97	1282.51	126.92	3.28	1133.52
4:03:20	1226.21	1357.69	1291.95	131.48	5.52	1050.83
4:06:40	1095.71	1268.84	1182.28	173.14	6.76	1056.32
4:10:00	1101.57	1262.99	1182.28	161.42	6.44	1002.35
4:13:20	1113.61	1257.13	1185.37	143.52	4.63	998.09
4:16:40	1130.21	1249.97	1190.09	119.76	2.03	986.87
4:20:00	1125.32	1249.97	1187.65	124.64	-0.45	1011.61
4:23:20	1128.90	1246.39	1187.65	117.48	-2.11	991.57
4:26:40	1150.38	1245.09	1197.73	94.70	-2.70	1012.02
4:30:00	1163.40	1246.39	1204.89	82.99	-2.32	996.50
4:33:20	1152.66	1236.95	1194.81	84.29	-1.17	1021.78
4:36:40	1165.68	1232.07	1198.87	66.39	0.49	1038.68
4:40:00	1162.10	1237.93	1200.01	75.83	2.24	992.25
4:43:20	1171.54	1233.37	1202.45	61.83	3.49	1056.93
4:46:40	1108.73	1234.35	1171.54	125.62	3.65	1053.13
4:50:00	1117.19	1291.30	1204.24	174.11	2.50	1004.80
4:53:20	1038.76	1207.34	1123.05	168.58	0.49	979.81
4:56:40	1057.63	1203.76	1130.69	146.12	-1.35	1079.29
5:00:00	1120.77	1278.28	1199.52	157.51	-1.95	981.60
5:03:20	1144.20	1276.98	1210.59	132.78	-0.81	986.03
5:06:40	1123.05	1272.42	1197.73	149.38	1.63	943.75
5:10:00	1049.50	1191.71	1120.60	142.22	4.29	1059.65
5:13:20	1064.79	1177.39	1121.09	112.60	6.03	915.39
5:16:40	1064.79	1164.38	1114.58	99.59	6.32	938.67
5:20:00	1063.81	1172.84	1118.33	109.02	5.34	929.60
5:23:20	1030.62	1166.98	1098.80	136.36	3.74	978.11
5:26:40	987.66	1171.54	1079.60	183.88	2.18	940.64
5:30:00	988.96	1154.94	1071.95	165.98	1.03	923.96
5:33:20	988.96	1143.22	1066.09	154.26	0.37	911.43
5:36:40	1006.86	1137.37	1072.11	130.50	0.11	917.77
5:40:00	1009.14	1151.36	1080.25	142.22	0.13	885.05
5:43:20	1010.44	1138.34	1074.39	127.90	0.24	822.89
5:46:40	1012.72	1130.21	1071.46	117.48	0.17	914.35
5:50:00	1006.86	1128.90	1067.88	122.04	-0.37	1044.51
5:53:20	1051.77	1201.15	1126.46	149.38	-1.36	912.29
5:56:40	980.83	1127.60	1054.21	146.77	-2.36	895.79
6:00:00	985.38	1124.02	1054.70	138.64	-2.62	954.43
6:03:20	1035.18	1206.03	1120.60	170.86	-1.56	926.78
6:06:40	1038.76	1191.71	1115.23	152.96	0.76	1005.96

6:10:00	1064.79	1183.58	1124.18	118.79	3.50	862.96
6:13:20	967.81	1102.87	1035.34	135.06	5.39	860.01
6:16:40	964.23	1099.29	1031.76	135.06	5.49	784.80
6:20:00	959.35	1105.15	1032.25	145.80	3.73	839.79
6:23:20	998.40	1100.59	1049.50	102.19	0.97	875.90
6:26:40	998.40	1107.42	1052.91	109.02	-1.52	853.30
6:30:00	1004.26	1099.29	1051.77	95.03	-2.73	818.39
6:33:20	997.42	1097.01	1047.22	99.59	-2.42	882.85
6:36:40	1015.00	1093.43	1054.21	78.43	-1.14	926.35
6:40:00	1024.44	1092.13	1058.28	67.69	0.23	910.36
6:43:20	1032.90	1087.57	1060.24	54.67	0.99	982.22
6:46:40	1027.04	1079.11	1053.08	52.07	0.94	914.73
6:50:00	1047.22	1073.25	1060.24	26.04	0.40	876.72
6:53:20	NaN	NaN	NaN	NaN	NaN	828.50
6:56:40	966.51	1131.18	1048.84	164.67	NaN	880.28
7:00:00	NaN	NaN	NaN	NaN	NaN	824.88
7:03:20	959.35	1107.42	1033.39	148.08	NaN	893.63
7:06:40	958.05	1120.77	1039.41	162.72	3.51	858.21
7:10:00	973.67	1106.45	1040.06	132.78	4.49	823.84
7:13:20	946.33	1022.16	984.24	75.83	4.81	822.56
7:16:40	947.63	1015.00	981.32	67.37	4.57	855.77
7:20:00	937.87	994.82	966.34	56.95	4.10	889.06
7:23:20	926.15	981.80	953.98	55.65	3.69	768.92
7:26:40	923.87	975.95	949.91	52.07	3.34	778.13
7:30:00	914.44	983.11	948.77	68.67	2.68	769.11
7:33:20	909.55	974.64	942.10	65.09	1.23	750.55
7:36:40	911.83	973.67	942.75	61.83	-1.13	702.68
7:40:00	907.28	964.23	935.75	56.95	-3.90	710.96
7:43:20	896.54	958.05	927.29	61.51	-6.02	847.31
7:46:40	1028.02	1066.09	1047.05	38.08	-6.41	893.48
7:50:00	980.83	1043.64	1012.23	62.81	-4.61	942.26
7:53:20	971.06	1037.78	1004.42	66.72	-1.16	843.60
7:56:40	959.35	1029.32	994.33	69.97	2.61	663.07
8:00:00	NaN	NaN	NaN	NaN	NaN	630.94
8:03:20	NaN	NaN	NaN	NaN	NaN	664.99
8:06:40	NaN	NaN	NaN	NaN	NaN	678.50
8:10:00	NaN	NaN	NaN	NaN	NaN	661.20
8:13:20	NaN	NaN	NaN	NaN	NaN	665.20
8:16:40	NaN	NaN	NaN	NaN	NaN	689.23

8:20:00	NaN	NaN	NaN	NaN	NaN	725.24
8:23:20	NaN	NaN	NaN	NaN	NaN	734.68
8:26:40	NaN	NaN	NaN	NaN	NaN	716.19
8:30:00	806.39	903.70	855.04	97.31	NaN	778.22
8:33:20	786.21	884.82	835.52	98.61	2.85	846.93
8:36:40	782.63	884.82	833.73	102.19	1.40	798.64
8:40:00	781.66	878.64	830.15	96.98	0.68	731.96
8:43:20	NaN	NaN	NaN	NaN	NaN	750.82
8:46:40	799.23	869.20	834.21	69.97	NaN	692.18
8:50:00	801.83	863.34	832.59	61.51	0.54	709.86
8:53:20	NaN	NaN	NaN	NaN	NaN	715.65
8:56:40	NaN	NaN	NaN	NaN	NaN	696.61

Table 2: Time series data for the shallow slope, fast RSL rise experiment.

Run: Shallow Low

Time (HH:MM:SS)	Landward Shoreline Distance (mm)	Basinward Shoreline Distance (mm)	Island Middle Distance (mm)	Island Width (mm)	Island Middle Velocity (mm/min)	Delta Radius (mm)
0:00:00	NaN	NaN	NaN	NaN	NaN	2049.53
0:05:00	NaN	NaN	NaN	NaN	NaN	1959.35
0:10:00	NaN	NaN	NaN	NaN	NaN	2062.92
0:15:00	NaN	NaN	NaN	NaN	NaN	2046.13
0:20:00	NaN	NaN	NaN	NaN	NaN	2075.58
0:25:00	NaN	NaN	NaN	NaN	NaN	2067.82
0:30:00	NaN	NaN	NaN	NaN	NaN	2057.63
0:35:00	NaN	NaN	NaN	NaN	NaN	2053.63
0:40:00	NaN	NaN	NaN	NaN	NaN	2061.05
0:45:00	NaN	NaN	NaN	NaN	NaN	2019.27
0:50:00	NaN	NaN	NaN	NaN	NaN	2019.77
0:55:00	NaN	NaN	NaN	NaN	NaN	1993.03
1:00:00	NaN	NaN	NaN	NaN	NaN	1989.07
1:05:00	NaN	NaN	NaN	NaN	NaN	1995.06
1:10:00	NaN	NaN	NaN	NaN	NaN	1993.66
1:15:00	NaN	NaN	NaN	NaN	NaN	2009.83
1:20:00	NaN	NaN	NaN	NaN	NaN	2017.90
1:25:00	NaN	NaN	NaN	NaN	NaN	2029.37
1:30:00	NaN	NaN	NaN	NaN	NaN	1946.18
1:35:00	NaN	NaN	NaN	NaN	NaN	2047.33
1:40:00	NaN	NaN	NaN	NaN	NaN	1911.71
1:45:00	NaN	NaN	NaN	NaN	NaN	1903.91
1:50:00	NaN	NaN	NaN	NaN	NaN	1847.70
1:55:00	NaN	NaN	NaN	NaN	NaN	1819.32
2:00:00	NaN	NaN	NaN	NaN	NaN	1814.77
2:05:00	NaN	NaN	NaN	NaN	NaN	1829.93
2:10:00	NaN	NaN	NaN	NaN	NaN	1860.15
2:15:00	NaN	NaN	NaN	NaN	NaN	1834.03
2:20:00	NaN	NaN	NaN	NaN	NaN	1880.39
2:25:00	NaN	NaN	NaN	NaN	NaN	2011.48
2:30:00	NaN	NaN	NaN	NaN	NaN	1937.84
2:35:00	NaN	NaN	NaN	NaN	NaN	1951.17
2:40:00	NaN	NaN	NaN	NaN	NaN	1927.59

2:45:00	NaN	NaN	NaN	NaN	NaN	1962.53
2:50:00	NaN	NaN	NaN	NaN	NaN	1906.37
2:55:00	NaN	NaN	NaN	NaN	NaN	1849.94
3:00:00	NaN	NaN	NaN	NaN	NaN	1861.03
3:05:00	NaN	NaN	NaN	NaN	NaN	1854.45
3:10:00	NaN	NaN	NaN	NaN	NaN	1900.07
3:15:00	NaN	NaN	NaN	NaN	NaN	1850.42
3:20:00	NaN	NaN	NaN	NaN	NaN	1876.08
3:25:00	NaN	NaN	NaN	NaN	NaN	1882.82
3:30:00	NaN	NaN	NaN	NaN	NaN	1872.82
3:35:00	NaN	NaN	NaN	NaN	NaN	1770.89
3:40:00	2170.05	2226.36	2198.21	56.30	NaN	1758.12
3:45:00	2187.63	2214.64	2201.13	27.01	0.51	1731.01
3:50:00	2172.98	2209.76	2191.37	36.78	2.55	1746.20
3:55:00	2113.75	2208.78	2161.27	95.03	3.93	1753.42
4:00:00	2098.13	2196.09	2147.11	97.96	3.78	1733.01
4:05:00	2077.63	2193.49	2135.56	115.86	2.42	1723.82
4:10:00	2088.37	2179.82	2134.09	91.45	0.97	1722.09
4:15:00	2075.68	2180.79	2128.24	105.12	0.30	1762.53
4:20:00	2065.26	2184.70	2124.98	119.44	0.21	1738.70
4:25:00	2074.70	2189.58	2132.14	114.88	-0.08	1799.10
4:30:00	2073.72	2184.70	2129.21	110.98	-0.87	1804.20
4:35:00	2104.97	2183.72	2144.34	78.76	-1.53	1705.60
4:40:00	2115.71	2178.84	2147.27	63.14	-1.19	1709.84
4:45:00	2101.06	2173.96	2137.51	72.90	0.20	1664.29
4:50:00	2120.59	2173.96	2147.27	53.37	1.64	1731.70
4:55:00	2078.60	2167.13	2122.87	88.52	1.97	1623.46
5:00:00	2085.44	2156.39	2120.91	70.95	1.04	1577.46
5:05:00	2093.25	2158.34	2125.79	65.09	-0.15	1596.65
5:10:00	2090.32	2154.43	2122.38	64.11	-0.39	1599.65
5:15:00	2095.20	2154.43	2124.82	59.23	0.61	1613.21
5:20:00	2072.75	2146.62	2109.68	73.88	1.99	1560.51
5:25:00	2062.33	2138.81	2100.57	76.48	2.63	1634.55
5:30:00	2039.88	2131.33	2085.60	91.45	2.12	1648.53
5:35:00	2035.97	2134.91	2085.44	98.93	1.01	1624.61
5:40:00	2035.00	2129.37	2082.18	94.38	0.17	1537.66
5:45:00	2034.02	2130.35	2082.18	96.33	-0.01	1627.26
5:50:00	2035.00	2127.42	2081.21	92.43	0.22	1549.75
5:55:00	2035.97	2121.56	2078.77	85.59	0.32	1612.71

6:00:00	2044.76	2114.73	2079.74	69.97	0.05	1572.91
6:05:00	2053.55	2112.78	2083.16	59.23	-0.41	1610.66
6:10:00	2064.29	2105.94	2085.11	41.66	-0.69	1571.30
6:15:00	2062.33	2106.92	2084.63	44.59	-0.53	1609.97
6:20:00	2077.63	2098.13	2087.88	20.50	0.06	1579.07
6:25:00	2075.68	2095.20	2085.44	19.53	0.91	1598.77
6:30:00	NaN	NaN	NaN	NaN	NaN	1585.08
6:35:00	2029.14	2092.27	2060.71	63.14	NaN	1667.43
6:40:00	2012.54	2081.53	2047.04	68.99	2.69	1623.68
6:45:00	1996.27	2077.63	2036.95	81.36	2.27	1648.57
6:50:00	1990.41	2072.75	2031.58	82.34	1.31	1577.63
6:55:00	1988.46	2072.10	2030.28	83.64	0.31	1541.62
7:00:00	1985.53	2067.21	2026.37	81.69	-0.18	1616.50
7:05:00	1987.48	2068.19	2027.84	80.71	-0.08	1601.96
7:10:00	1993.34	2070.14	2031.74	76.80	0.12	1552.73
7:15:00	2002.13	2065.26	2033.69	63.14	-0.18	1523.31
7:20:00	1995.29	2070.14	2032.72	74.85	-0.89	1544.57
7:25:00	2013.52	2058.43	2035.97	44.91	-1.15	1547.68
7:30:00	2024.26	2058.43	2041.34	34.17	-0.13	1516.35
7:35:00	2026.21	2052.57	2039.39	26.36	1.88	1550.23
7:40:00	1973.81	2042.81	2008.31	68.99	3.49	1469.59
7:45:00	1958.19	2036.95	1997.57	78.76	3.37	1514.71
7:50:00	1947.78	2030.11	1988.95	82.34	1.65	1544.51
7:55:00	1959.17	2028.16	1993.66	68.99	-0.17	1511.77
8:00:00	1960.14	2012.54	1986.34	52.40	-0.53	1505.86
8:05:00	1962.10	2017.42	1989.76	55.33	0.68	1506.01
8:10:00	1971.86	2009.94	1990.90	38.08	2.13	1488.10
8:15:00	1908.72	1999.20	1953.96	90.47	2.43	1493.93
8:20:00	1902.87	2007.01	1954.94	104.14	1.36	1492.95
8:25:00	1932.16	2008.96	1970.56	76.80	-0.10	1482.48
8:30:00	1923.37	2010.91	1967.14	87.54	-0.93	1476.79
8:35:00	1920.44	2003.10	1961.77	82.66	-0.83	1406.77
8:40:00	1928.25	2012.54	1970.40	84.29	-0.20	1510.92
8:45:00	1941.92	1989.43	1965.68	47.51	0.54	1477.08
8:50:00	1948.75	1982.60	1965.68	33.85	1.23	1440.70
8:55:00	NaN	NaN	NaN	NaN	NaN	1460.06
9:00:00	1902.87	1978.69	1940.78	75.83	NaN	1482.05
9:05:00	1895.06	1978.69	1936.87	83.64	1.15	1445.47
9:10:00	1897.01	1976.74	1936.87	79.73	0.20	1452.34

9:15:00	1915.56	1970.88	1943.22	55.33	-0.52	1501.74
9:20:00	1921.42	1962.10	1941.76	40.68	-0.72	1461.53
9:25:00	1927.27	1964.05	1945.66	36.78	-0.55	1501.29
9:30:00	1932.16	1962.10	1947.13	29.94	-0.37	1457.56
9:35:00	1933.13	1964.05	1948.59	30.92	-0.26	1510.97
9:40:00	1937.04	1966.00	1951.52	28.96	-0.07	1462.85
9:45:00	1932.16	1961.12	1946.64	28.96	0.18	1479.34
9:50:00	1938.99	1960.14	1949.57	21.15	0.24	1531.66
9:55:00	1938.01	1955.26	1946.64	17.25	0.04	1541.75
10:00:00	1931.18	1958.19	1944.69	27.01	0.09	1501.17
10:05:00	1928.25	1951.36	1939.80	23.11	1.01	1510.37
10:10:00	1929.23	1948.75	1938.99	19.53	2.60	1546.10
10:15:00	1855.35	1941.92	1898.63	86.57	3.63	1558.71
10:20:00	1863.16	1937.04	1900.10	73.88	2.89	1473.27
10:25:00	1858.28	1936.06	1897.17	77.78	0.61	1475.50
10:30:00	1873.90	1920.44	1897.17	46.54	-1.42	1474.34
10:35:00	1890.17	1917.51	1903.84	27.34	-1.45	1473.46
10:40:00	1896.03	1917.51	1906.77	21.48	0.48	1546.67
10:45:00	1870.00	1924.34	1897.17	54.35	2.51	1517.99
10:50:00	1845.59	1908.72	1877.16	63.14	2.76	1506.40
10:55:00	1830.94	1907.75	1869.35	76.80	1.21	1505.55
11:00:00	1832.90	1904.82	1868.86	71.92	-0.39	1505.79
11:05:00	1863.16	1910.68	1886.92	47.51	-0.40	1559.40
11:10:00	1844.61	1901.89	1873.25	57.28	1.08	1528.24
11:15:00	1809.79	1891.15	1850.47	81.36	2.43	1516.03
11:20:00	1811.74	1879.76	1845.75	68.02	2.23	1513.95
11:25:00	1814.67	1885.62	1850.14	70.95	0.66	1485.62
11:30:00	NaN	NaN	NaN	NaN	NaN	1499.50
11:35:00	1819.55	1885.62	1852.58	66.06	NaN	1528.35
11:40:00	1823.46	1884.64	1854.05	61.18	-0.47	1552.68
11:45:00	1833.87	1882.69	1858.28	48.82	0.60	1536.45
11:50:00	1822.48	1871.95	1847.21	49.47	1.22	1518.82
11:55:00	1815.65	1872.92	1844.29	57.28	1.32	1534.86
12:00:00	1791.24	1876.83	1834.03	85.59	1.17	1555.56
12:05:00	1794.17	1870.00	1832.08	75.83	0.86	1526.44
12:10:00	1785.38	1871.95	1828.66	86.57	0.34	1505.42
12:15:00	1789.29	1877.81	1833.55	88.52	-0.24	1502.54
12:20:00	1794.17	1872.92	1833.55	78.76	-0.43	1487.03
12:25:00	1795.14	1869.02	1832.08	73.88	0.00	1507.50

12:30:00	1795.14	1862.19	1828.66	67.04	0.66	1516.22
12:35:00	1801.98	1856.33	1829.15	54.35	0.79	1538.28
12:40:00	1800.03	1850.47	1825.25	50.44	0.11	1569.43
12:45:00	1801.98	1851.45	1826.71	49.47	-0.70	1519.21
12:50:00	1812.72	1854.37	1833.55	41.66	-0.65	1543.02
12:55:00	1808.81	1857.30	1833.06	48.49	0.47	1532.88
13:00:00	1784.40	1845.59	1815.00	61.18	1.66	1500.82
13:05:00	1785.38	1849.49	1817.44	64.11	1.64	1495.36
13:10:00	1795.14	1836.80	1815.97	41.66	0.28	1489.95
13:15:00	1795.14	1833.87	1814.51	38.73	-1.10	1496.04
13:20:00	1800.03	1835.82	1817.93	35.80	-0.97	1519.84
13:25:00	1798.07	1837.78	1817.93	39.70	0.76	1523.21
13:30:00	1801.00	1837.78	1819.39	36.78	2.58	1540.79
13:35:00	1740.80	1827.04	1783.92	86.24	2.84	1514.83
13:40:00	1727.13	1825.41	1776.27	98.28	1.42	1527.11
13:45:00	1743.72	1839.73	1791.73	96.01	-0.28	1459.91
13:50:00	1764.23	1824.43	1794.33	60.21	-0.92	1449.12
13:55:00	1758.37	1826.39	1792.38	68.02	-0.58	1414.80
14:00:00	1764.23	1819.55	1791.89	55.33	-0.36	1522.08
14:05:00	NaN	NaN	NaN	NaN	NaN	1516.17
14:10:00	1791.24	1823.46	1807.35	32.22	NaN	1559.16
14:15:00	1795.14	1826.39	1810.77	31.24	-0.87	1540.14
14:20:00	1796.12	1818.58	1807.35	22.46	0.94	1552.09
14:25:00	1781.48	1816.62	1799.05	35.15	2.69	1458.10
14:30:00	1736.89	1799.05	1767.97	62.16	2.95	1511.56
14:35:00	1725.17	1809.79	1767.48	84.62	1.59	1545.17
14:40:00	1754.46	1813.69	1784.08	59.23	-0.21	1568.78
14:45:00	1730.06	1817.60	1773.83	87.54	-1.25	1480.66
14:50:00	1742.75	1816.62	1779.69	73.88	-1.36	1530.75
14:55:00	1763.25	1814.67	1788.96	51.42	-1.14	1509.33
15:00:00	1785.38	1814.67	1800.03	29.29	-0.95	1502.74
15:05:00	1781.48	1811.74	1796.61	30.27	-0.58	1500.09
15:10:00	1787.33	1801.98	1794.66	14.64	0.17	1505.05
15:15:00	1785.38	1801.00	1793.19	15.62	0.85	1509.56
15:20:00	1780.50	1799.05	1789.77	18.55	0.77	1452.49
15:25:00	1779.52	1799.05	1789.29	19.53	-0.09	1491.50
15:30:00	1778.55	1803.93	1791.24	25.38	-0.80	1401.19
15:35:00	1784.40	1805.88	1795.14	21.48	-0.40	1489.76
15:40:00	1781.48	1802.95	1792.22	21.48	1.01	1536.05

15:45:00	1770.74	1790.26	1780.50	19.53	2.21	1374.67
15:50:00	1741.77	1787.33	1764.55	45.56	2.14	1377.29
15:55:00	1736.89	1786.36	1761.62	49.47	1.00	1422.34
16:00:00	1738.84	1799.05	1768.95	60.21	0.05	1356.79
16:05:00	NaN	NaN	NaN	NaN	NaN	1354.52
16:10:00	NaN	NaN	NaN	NaN	NaN	1522.16
16:15:00	NaN	NaN	NaN	NaN	NaN	1521.64
16:20:00	NaN	NaN	NaN	NaN	NaN	1528.68
16:25:00	1678.64	1770.74	1724.69	92.10	NaN	1530.32
16:30:00	1679.61	1765.85	1722.73	86.24	0.15	1559.11
16:35:00	1690.35	1767.81	1729.08	77.46	-0.12	1555.40
16:40:00	1670.82	1773.66	1722.24	102.84	-0.05	1493.46
16:45:00	1685.47	1774.64	1730.06	89.17	-0.27	1427.87
16:50:00	1693.28	1769.76	1731.52	76.48	-0.78	1365.11
16:55:00	1704.67	1761.30	1732.98	56.63	-0.97	1343.39
17:00:00	1706.62	1765.85	1736.24	59.23	-0.41	1305.84
17:05:00	1718.34	1764.88	1741.61	46.54	0.49	1375.78
17:10:00	1710.53	1751.53	1731.03	41.01	0.89	1373.22
17:15:00	1696.21	1747.63	1721.92	51.42	0.47	1412.18
17:20:00	1703.04	1763.25	1733.15	60.21	-0.19	1469.42
17:25:00	1708.58	1755.44	1732.01	46.86	-0.28	1485.63
17:30:00	1711.51	1747.63	1729.57	36.12	0.27	1471.58
17:35:00	1708.58	1747.63	1728.10	39.05	0.72	1461.75
17:40:00	1691.33	1745.68	1718.50	54.35	0.42	1477.64
17:45:00	1708.58	1750.56	1729.57	41.98	-0.29	1491.11
17:50:00	1711.51	1742.75	1727.13	31.24	-0.41	1488.55
17:55:00	1708.58	1738.84	1723.71	30.27	0.48	1486.04
18:00:00	1709.55	1730.06	1719.80	20.50	1.65	1497.70
18:05:00	1673.75	1735.91	1704.83	62.16	1.91	1479.33
18:10:00	1670.82	1735.91	1703.37	65.09	0.93	1469.00
18:15:00	1668.87	1739.82	1704.35	70.95	-0.37	1488.17
18:20:00	1676.68	1738.84	1707.76	62.16	-0.80	1453.66
18:25:00	1682.54	1741.77	1712.16	59.23	-0.23	1460.51
18:30:00	1682.54	1732.98	1707.76	50.44	0.40	1438.89
18:35:00	1680.59	1727.13	1703.86	46.54	0.20	1415.68
18:40:00	1691.33	1731.03	1711.18	39.70	-0.59	1437.15
18:45:00	NaN	NaN	NaN	NaN	NaN	1403.42
18:50:00	1700.11	1732.98	1716.55	32.87	NaN	1470.19
18:55:00	1704.67	1724.20	1714.43	19.53	0.81	1463.28

19:00:00	1693.28	1712.48	1702.88	19.20	1.24	1408.78
19:05:00	1668.87	1732.01	1700.44	63.14	0.58	1459.79
19:10:00	1675.71	1738.84	1707.27	63.14	-0.51	1450.46
19:15:00	1686.45	1738.84	1712.64	52.40	-0.98	1409.82
19:20:00	1688.40	1736.89	1712.64	48.49	-0.54	1427.45
19:25:00	1684.49	1732.01	1708.25	47.51	0.20	1505.58
19:30:00	1692.30	1728.10	1710.20	35.80	0.46	1488.99
19:35:00	1701.09	1720.29	1710.69	19.20	0.10	1396.04
19:40:00	NaN	NaN	NaN	NaN	NaN	1452.33
19:45:00	1687.42	1735.91	1711.67	48.49	NaN	1371.38
19:50:00	1688.40	1731.03	1709.72	42.63	0.32	1316.40
19:55:00	1686.45	1727.13	1706.79	40.68	1.26	1345.48
20:00:00	1661.06	1722.24	1691.65	61.18	1.96	1414.13
20:05:00	1648.37	1724.20	1686.28	75.83	2.02	1439.49
20:10:00	1647.39	1710.53	1678.96	63.14	1.29	1431.82
20:15:00	1647.39	1707.60	1677.50	60.21	0.13	1434.41
20:20:00	1660.09	1702.07	1681.08	41.98	-0.76	1401.22
20:25:00	1664.97	1699.14	1682.05	34.17	-0.64	1440.40
20:30:00	1656.18	1703.69	1679.94	47.51	0.56	1460.39
20:35:00	1660.09	1705.65	1682.87	45.56	2.09	1451.19

Table 3: Time series data for the shallow slope, slow RSL rise experiment.

Run: Steep Fast

Time (HH:MM:SS)	Landward Shoreline Distance (mm)	Basinward Shoreline Distance (mm)	Island Middle Distance (mm)	Island Width (mm)	Island Middle Velocity (mm/min)	Delta Radius (mm)
0:00:00	1795.58	1845.38	1820.48	49.79	NaN	1877.10
0:02:00	1795.25	1779.10	1787.17	16.15	7.30	1887.42
0:04:00	1751.51	1834.27	1792.89	82.76	6.52	1767.99
0:06:00	1754.87	1835.95	1795.41	81.08	5.49	1715.23
0:08:00	1758.24	1837.64	1797.94	79.40	4.34	1713.36
0:10:00	1762.95	1837.64	1800.29	74.69	3.21	1716.86
0:12:00	1743.77	1844.37	1794.07	100.60	2.23	1592.67
0:14:00	1737.04	1831.58	1784.31	94.54	1.48	1740.86
0:16:00	1746.80	1837.64	1792.22	90.84	0.99	1742.14
0:18:00	1745.12	1821.15	1783.13	76.04	0.77	1644.95
0:20:00	1701.72	1829.23	1765.47	127.51	0.76	1700.36
0:22:00	1701.72	1819.81	1760.76	118.09	0.87	1735.73
0:24:00	1698.01	1811.39	1754.70	113.38	1.02	1711.64
0:26:00	1703.06	1818.12	1760.59	115.06	1.12	1734.16
0:28:00	1704.74	1813.08	1758.91	108.33	1.13	1758.72
0:30:00	1717.53	1827.88	1772.70	110.35	1.02	1644.48
0:32:00	1712.82	1822.83	1767.83	110.02	0.79	1649.94
0:34:00	1712.82	1826.20	1769.51	113.38	0.49	1696.95
0:36:00	1703.06	1819.47	1761.27	116.41	0.16	1724.85
0:38:00	1698.01	1814.76	1756.39	116.74	-0.14	1711.40
0:40:00	1720.89	1811.39	1766.14	90.50	-0.36	1460.11
0:42:00	1707.77	1811.39	1759.58	103.62	-0.48	1679.39
0:44:00	1714.16	1806.68	1760.42	92.52	-0.50	1638.21
0:46:00	1710.80	1803.66	1757.23	92.86	-0.43	1714.57
0:48:00	1722.57	1796.93	1759.75	74.35	-0.31	1687.65
0:50:00	1734.01	1824.52	1779.26	90.50	-0.18	1567.04
0:52:00	1734.01	1806.68	1770.35	72.67	-0.10	1601.32
0:54:00	1738.72	1798.61	1768.67	59.89	-0.08	1612.44
0:56:00	1724.26	1810.05	1767.15	85.79	-0.14	1697.10
0:58:00	1717.53	1805.34	1761.43	87.81	-0.26	1707.74
1:00:00	1714.84	1816.78	1765.81	101.94	-0.41	1601.46
1:02:00	1717.86	1813.08	1765.47	95.21	-0.54	1659.55
1:04:00	NaN	NaN	NaN	NaN	NaN	1703.90

1:06:00	NaN	NaN	NaN	NaN	NaN	1677.61
1:08:00	1727.28	1811.39	1769.34	84.11	NaN	1708.23
1:10:00	1738.72	1819.47	1779.10	80.75	-0.09	1540.57
1:12:00	1740.41	1818.12	1779.26	77.72	0.32	1596.33
1:14:00	1738.72	1811.39	1775.06	72.67	0.78	1606.15
1:16:00	1738.39	1808.37	1773.38	69.98	1.23	1611.12
1:18:00	1734.01	1811.73	1772.87	77.72	1.61	1641.70
1:20:00	1669.42	1809.71	1739.56	140.30	1.87	1534.39
1:22:00	1693.30	1803.66	1748.48	110.35	1.96	1510.25
1:24:00	1698.01	1802.31	1750.16	104.30	1.86	1547.86
1:26:00	1703.06	1800.29	1751.68	97.23	1.59	1567.41
1:28:00	1672.11	1803.32	1737.71	131.21	1.17	1538.66
1:30:00	1701.72	1810.05	1755.88	108.33	0.64	1424.47
1:32:00	1704.74	1798.61	1751.68	93.87	0.07	1354.95
1:34:00	1701.72	1795.25	1748.48	93.53	-0.50	1312.08
1:36:00	1703.06	1800.29	1751.68	97.23	-1.01	1414.73
1:38:00	1712.82	1785.83	1749.32	73.01	-1.45	1556.67
1:40:00	NaN	NaN	NaN	NaN	NaN	1613.11
1:42:00	NaN	NaN	NaN	NaN	NaN	1675.07
1:44:00	NaN	NaN	NaN	NaN	NaN	1656.83
1:46:00	NaN	NaN	NaN	NaN	NaN	1673.89
1:48:00	NaN	NaN	NaN	NaN	NaN	1684.78
1:50:00	1734.01	1821.15	1777.58	87.14	NaN	1594.38
1:52:00	1730.31	1822.83	1776.57	92.52	-2.46	1602.80
1:54:00	1742.09	1819.81	1780.95	77.72	-2.52	1622.73
1:56:00	1749.83	1849.41	1799.62	99.59	-2.58	1501.01
1:58:00	NaN	NaN	NaN	NaN	NaN	1623.94
2:00:00	NaN	NaN	NaN	NaN	NaN	1646.75
2:02:00	NaN	NaN	NaN	NaN	NaN	1635.85
2:04:00	NaN	NaN	NaN	NaN	NaN	1518.67
2:06:00	NaN	NaN	NaN	NaN	NaN	1602.75
2:08:00	NaN	NaN	NaN	NaN	NaN	1611.33
2:10:00	1780.78	1874.65	1827.71	93.87	NaN	1525.46
2:12:00	1777.41	1878.01	1827.71	100.60	-1.29	1537.91
2:14:00	1777.41	1869.94	1823.67	92.52	-0.75	1521.99
2:16:00	1784.14	1874.65	1829.39	90.50	-0.15	1499.56
2:18:00	NaN	NaN	NaN	NaN	NaN	1520.84
2:20:00	1788.85	1874.65	1831.75	85.79	NaN	1409.55
2:22:00	1785.83	1866.57	1826.20	80.75	1.59	1487.99

2:24:00	1784.14	1868.59	1826.37	84.45	2.01	1427.87
2:26:00	1782.46	1866.57	1824.52	84.11	2.31	1545.48
2:28:00	1783.81	1863.21	1823.51	79.40	2.47	1529.53
2:30:00	1741.75	1852.10	1796.93	110.35	2.49	1542.14
2:32:00	1739.06	1850.42	1794.74	111.36	2.37	1561.15
2:34:00	1735.36	1852.10	1793.73	116.74	2.15	1530.35
2:36:00	1738.72	1844.03	1791.38	105.31	1.86	1601.82
2:38:00	1737.04	1839.32	1788.18	102.28	1.53	1559.54
2:40:00	1740.07	1840.66	1790.37	100.60	1.22	1514.51
2:42:00	1731.99	1842.35	1787.17	110.35	0.94	1451.61
2:44:00	1733.68	1840.66	1787.17	106.99	0.71	1524.41
2:46:00	1735.36	1845.71	1790.54	110.35	0.55	1552.70
2:48:00	1734.01	1844.03	1789.02	110.02	0.45	1582.55
2:50:00	1712.82	1837.64	1775.23	124.82	0.39	1508.42
2:52:00	1706.09	1835.95	1771.02	129.87	0.37	1507.18
2:54:00	1712.82	1837.64	1775.23	124.82	0.35	1505.80

Table 4: Time series data for the steep slope, fast RSL rise experiment.

Run: Steep Slow

Time (HH:MM:SS)	Landward Shoreline Distance (mm)	Basinward Shoreline Distance (mm)	Island Middle Distance (mm)	Island Width (mm)	Island Middle Velocity (mm/min)	Delta Radius (mm)
0:00:00	1341.94	1396.39	1369.17	54.45	NaN	1265.75
0:05:00	1334.48	1389.68	1362.08	55.20	0.21	1268.71
0:10:00	1332.99	1391.17	1362.08	58.18	0.74	1279.19
0:15:00	1331.50	1381.48	1356.49	49.98	1.11	1244.88
0:20:00	1328.51	1376.25	1352.38	47.74	1.12	1253.88
0:25:00	1324.04	1374.76	1349.40	50.72	0.76	1246.74
0:30:00	1325.53	1365.06	1345.30	39.53	0.26	1221.86
0:35:00	1324.78	1370.29	1347.54	45.50	-0.08	1199.06
0:40:00	1325.53	1363.57	1344.55	38.04	-0.07	1178.32
0:45:00	1321.80	1371.03	1346.42	49.23	0.32	1195.93
0:50:00	1324.04	1365.81	1344.92	41.77	0.90	1184.55
0:55:00	1317.32	1351.64	1334.48	34.31	1.45	1196.61
1:00:00	1294.20	1339.70	1316.95	45.50	1.74	1193.92
1:05:00	1279.28	1359.10	1319.19	79.82	1.62	1125.26
1:10:00	1276.30	1355.37	1315.83	79.07	1.07	1195.99
1:15:00	1268.84	1353.88	1311.36	85.04	0.19	1147.65
1:20:00	1282.27	1335.23	1308.75	52.96	-0.68	1143.41
1:25:00	1286.00	1358.35	1322.17	72.36	-1.14	1090.08
1:30:00	1298.68	1350.89	1324.78	52.22	-0.93	1138.02
1:35:00	1300.17	1352.38	1326.28	52.22	-0.23	1091.37
1:40:00	1294.20	1349.40	1321.80	55.20	0.42	1114.96
1:45:00	1297.93	1348.65	1323.29	50.72	0.52	1094.46
1:50:00	1293.45	1351.64	1322.55	58.18	0.03	1101.07
1:55:00	1294.20	1346.42	1320.31	52.22	-0.49	1099.49
2:00:00	1298.68	1349.40	1324.04	50.72	-0.28	1086.90
2:05:00	1291.96	1344.18	1318.07	52.22	0.88	1074.77
2:10:00	1294.20	1341.19	1317.70	46.99	2.35	1066.63
2:15:00	1241.99	1341.19	1291.59	99.21	3.03	1071.06
2:20:00	1215.88	1330.01	1272.94	114.13	2.17	1059.74
2:25:00	1233.78	1338.21	1286.00	104.43	0.12	1032.28
2:30:00	1250.94	1338.21	1294.57	87.27	-1.92	1094.60
2:35:00	1271.82	1337.47	1304.64	65.64	-2.71	1048.65
2:40:00	1286.00	1339.70	1312.85	53.71	-1.95	1063.04

2:45:00	1294.20	1337.47	1315.83	43.26	-0.41	1064.33
2:50:00	1288.23	1339.70	1313.97	51.47	0.71	1209.72
2:55:00	1286.00	1339.70	1312.85	53.71	0.79	1170.86
3:00:00	1276.30	1335.97	1306.14	59.67	0.15	1135.08
3:05:00	1282.27	1337.47	1309.87	55.20	-0.40	1159.99
3:10:00	1291.96	1333.74	1312.85	41.77	-0.33	1135.24
3:15:00	1291.96	1335.23	1313.60	43.26	0.19	1112.79
3:20:00	1283.01	1327.02	1305.02	44.01	0.61	1110.32
3:25:00	1286.00	1333.74	1309.87	47.74	0.57	1064.17
3:30:00	1283.01	1324.78	1303.90	41.77	0.28	1064.12
3:35:00	1279.28	1321.80	1300.54	42.52	0.18	1064.23
3:40:00	1286.74	1314.34	1300.54	27.60	0.41	1099.66
3:45:00	1290.47	1312.10	1301.29	21.63	0.60	1127.50
3:50:00	1274.81	1321.05	1297.93	46.25	0.31	1143.36
3:55:00	1277.04	1321.05	1299.05	44.01	-0.41	1047.43
4:00:00	1279.28	1318.07	1298.68	38.79	-0.89	1035.59
4:05:00	1284.50	1320.31	1302.41	35.80	-0.37	1056.04
4:10:00	1288.23	1323.29	1305.76	35.06	1.19	1071.21
4:15:00	1268.84	1307.63	1288.23	38.79	2.92	1041.42
4:20:00	1218.12	1302.41	1260.26	84.29	3.54	1102.12
4:25:00	1200.21	1306.14	1253.17	105.92	2.42	1120.51
4:30:00	1200.21	1301.66	1250.94	101.45	0.11	968.43
4:35:00	1233.78	1302.41	1268.09	68.63	-2.04	1032.21
4:40:00	1258.40	1311.36	1284.88	52.96	-2.82	1087.89
4:45:00	1261.38	1305.39	1283.38	44.01	-2.05	1034.46
4:50:00	1265.11	1308.37	1286.74	43.26	-0.53	1083.95
4:55:00	1265.86	1309.12	1287.49	43.26	0.60	1040.41
5:00:00	1269.58	1312.85	1291.22	43.26	0.73	1013.50
5:05:00	1268.09	1300.17	1284.13	32.08	0.12	993.02
5:10:00	1272.57	1299.42	1286.00	26.85	-0.50	1095.31
5:15:00	1271.08	1300.17	1285.62	29.09	-0.57	1086.38
5:20:00	1274.81	1306.14	1290.47	31.33	-0.06	1092.99
5:25:00	1274.81	1303.15	1288.98	28.35	0.56	1028.25
5:30:00	1256.90	1306.88	1281.89	49.98	0.80	1086.43
5:35:00	1261.38	1307.63	1284.50	46.25	0.48	1067.44
5:40:00	1258.40	1294.20	1276.30	35.80	-0.15	1082.66
5:45:00	1258.40	1302.41	1280.40	44.01	-0.62	1090.78

Table 5: Time series data for the steep slope, slow RSL rise experiment.